NASA CR 137705

OPTIMUM PERFORMANCE AND POTENTIAL FLOW FIELD OF HOVERING ROTORS

By J. C. Wu and R. K. Sigman

Georgia Institute of Technology

Atlanta, Georgia

Prepared for

The U. S. Army

Air Mobility Research and Development Laboratory

NASA Ames Research Center

Grant No. NASA-6340

May 1975

NASA CR 137705

OPTIMUM PERFORMANCE AND POTENTIAL FLOW FIELD OF HOVERING ROTORS

By J. C. Wu and R. K. Sigman

May 1975

A Final Report Prepared under Contract No. NASA-6340 by

The Georgia Institute of Technology
Atlanta, Georgia

for

The U. S. Army

Air Mobility Research and Development Laboratory

Ames Directorate

Ames Research Center

National Aeronautics and Space Administration

TABLE OF CONTENTS

SUMMARY

Studies of rotor and propeller performance and induced potential flowfields are made on the basis of a rotating actuator disk concept, with special emphasis placed on rotors hovering out of ground effect. A new theory for the optimum performance of rotors hovering OGE is developed and presented. An extended theory for the optimum performance of rotors and propellers in axial motion is also presented. Numerical results are presented for the optimum distributions of blade-bound circulation together with axial inflow and ultimate wake velocities for the hovering rotor over the range of thrust coefficient of interest in rotorcraft applications. Shapes of the stream tubes and of the velocities in the slipstream are obtained, using available methods, for optimum and "off-optimum" circulation distributions for rotors hovering in and out of ground effect. Results of the optimum performance study show that improvements made possible by the present performance theory, which fully account for the effects of slipstream rotation, is important to the optimum circulation as well as to the power and the thrust requirements of the rotor in the higher thrust coefficient range. A number of explicit formulae useful in computing rotor and propeller induced flows are presented for stream functions and velocities due to distributions of circular vortices over axi-symmetric surfaces. The computed slipstream shape shows that the assumption of a uniform contraction ratio is reasonable and that, within the limitations of the infinitely bladed model, the computed results provide a reasonable description of the wake boundary.

NOMENCLATURE

a	radial location of perturbation in the ultimate wake
c	contraction ratio
C_P	power coefficient defined in Eq. (56)
C_T	thrust coefficient defined in Eq. (55)
D	domain of integration consisting of the rotor slipstream
$\vec{e}$	unit vector
E	complete elliptic integral of the second kind
F	function defined in Eq. (B-10)
$\vec{F}$	body force vector
G	Green's function for the streamfunction defined by Eq. (23)
G_r	Green's function for the axial velocity defined by Eq. (77)
h	function defined by Eqs. (43) and (B-6)
H	total head of the fluid
k	modulus of elliptic integrals
k_1	modulus defined by Eq. (A-26)
k_2	modulus defined by Eq. (A-27)
k_{r_1}	modulus defined by Eq. (A-54)
k_{r_2}	modulus defined by Eq. (A-55)
K	complete elliptic integral of the first kind
ℓ	indicates the ℓ^{th} segment of constant circulation
L	total number of segments of constant circulation
m_1	characteristic defined by Eq. (A-51)
m_2	characteristic defined by Eq. (A-52)
M	figure of merit defined by Eq. (54)

n	the "characteristic" of elliptic integrals of the third kind
$\vec{n}$	unit outward normal vector to the control volume
N	a constant defined by Eq. (45)
p	static pressure of the fluid
P	power expended by the rotor
$\vec{q}$	velocity vector
r	radial coordinate in a cylindrical coordinate system
$\vec{r}$	position vector of an observation point
r_1	inner radius of an annular surface
r_2	outer radius of an annular surface
r'	position vector of a vortex filament
R	radial location of a vortex filament
R_d	radius of the rotor or propeller disk
R_ℓ	radial location of the ℓ^{th} discontinuity in disk circulation
R_w	radius of the slipstream in the ultimate wake
$\mathcal{R}$	radius of a control volume centered at the rotor hub
s	annular element of area
$\vec{s}$	arc length of a vortex segment
S_1	the portion of the control surface which is cut out by the wake slipstream
S_2	the portion of the control surface excluding S_1
t	time
T	thrust of the rotor
u	radial component of the velocity
v	tangential component of the velocity
w	axial component of the velocity

W	constant value of the axial velocity in the ultimate wake within a streamtube of constant circulation
x	is defined as k_1^2
z	axial coordinate in a cylindrical coordinate system
Z	axial location of a vortex filament
α	variable of integration of elliptic integrals
γ	vortex strength per unit length
Γ	bound circulation at the disk
δ	function defined by Eq. (A-12)
Δ	indicates a perturbed value in the ultimate wake
ϵ	perturbed value of the angular velocity in the ultimate wake
ζ	axial component of vorticity
η	tangential component of vorticity
θ	tangential coordinate in a cylindrical coordinate system
κ	vortex filament strength
λ	vortex strength per unit length
λ_1	constant in Eq. (A-43) defining a linear vortex strength
λ_2	constant in Eq. (A-43) defining a linear vortex strength
λ_3	constant for vortex strength on an annular surface
Λ	advance ratio defined as $w_\infty/\Omega R_d$
ξ	radial component of the vorticity
Π	complete elliptic integral of the third kind
ρ	density of the fluid
Ψ	stream function
$\vec{\omega}$	vorticity vector
Ω	angular velocity of the rotor

Superscripts

'	indicates a variable of integration
~	denotes a dimensionless variable defined by Eq. (49)

Subscripts

d	denotes a variable at the rotor disk
f	refers to a quantity induced by a circular vortex filament
m	indicates a value on the m^{th} vortex tube
w	refers to a value in the ultimate wake
o	indicates a variable at the rim of the slipstream in the ultimate wake
∞	denotes a value in the undisturbed freestream

1. INTRODUCTION

The development of a suitable theory for predicting the flow field induced by a rotor has long been a central problem of rotorcraft aerodynamics. Since the flowfield induced by the rotor is ultimately responsible for the aerodynamic and dynamic behaviors of the rotorcraft, improvements in methods for predicting the flowfield contribute to the advancement of rotorcraft design in various ways.

The case of a rotor in hover is of special importance in a number of practical problems. These problems include the familiar operational problems, the problem of downwash impingement which leads to a ground boundary layer and particle entrainment, the problem of tail rotor behavior when immersed in the slipstream of a main rotor, and the problem of rotor performance. The general subject of a rotor in forward flight involves, of course, many additional important problems and is more complicated than the hovering case. It is generally expected that a thorough understanding of the latter will precede and then contribute substantially to research of the former. The hovering case, however, is in itself of such complexity that a theory sufficiently accurate and yet simple enough to be used as a design tool is yet unavailable. The development of such a theory is emphasized in the current literature.

A hovering rotor is a special case of a propeller, with zero advance velocity. Marine and aircraft engineers have long been concerned with propeller aerodynamics. In the majority of situations of

interest to the propeller aerodynamicist, however, the propeller-induced velocity is small in comparison with the propeller's velocity of advance. As a consequence, the propeller aerodynamicist is accustomed to simplifications that are not necessarily valid for the hovering rotor problem. Propeller theories therefore do not usually go over to rotor theories in a straight forward manner and predictions based on generalized propeller theories do not always correlate well with experimental data for rotors (Ref. 1).

Of the several problems mentioned earlier, the problem of predicting the rotor performance in hover out of ground effect (OGE) is particularly important. Rotorcraft are typically required to be able to hover OGE when occasion demands. Since the power required for a rotor to develop a given amount of thrust is the greatest during hover OGE, the payload capability of the rotorcraft is generally limited by the hovering performance OGE. Modern rotorcraft characteristically have small ratios of payload to gross weight at take off. Consequently, errors in the predicted hovering performance are amplified in the calculation of payload capability. For example, with a payload to gross weight ratio of 1/5 at take off, a 5% error in the prediction of hovering thrust means a 25% error in the predicted payload capability.

In recent years, a sizable effort has been in progress to establish suitably simple, yet sufficiently accurate theories and methods for predicting hovering rotor performance and induced flowfields. A review of the state of art of the hovering rotor problem is presented in Section II of this report. This review shows that, although recent progress in this area has been extensive, there still exists a need to

improve upon the available theories and methods for modern rotors with high rotational speed, solidity, and disk loading.

The purpose of this report is to present recent research results that serve to supplement the available theories and methods. In particular, an improved theory for the optimum performance of hovering rotors is presented. This theory is based on the actuator disk concept and therefore subject to some of the limitations of the well known general momentum theory. The correction factor for finite number of blades must be estimated separately, for example, by an extension of Lerbs' method (Ref. 2) for heavily loaded propellers. The improved theory, however, is more complete in that it fully accounts for the effects of slipstream rotation. This improvement is not important in the case of a lightly loaded rotor, but has finite contributions to thrust and to power requirements of a heavily loaded rotor. The improved theory permits the computation, in a straight forward manner, of the optimum distributions of circulation and inflow velocity over the rotor disk. These distributions, along with the figure of merit and the optimum power coefficient, are presented for several values of the thrust coefficient.

In addition to the optimum performance theory, flow fields induced by the infinitely bladed rotor hovering in, as well as out of, ground effect are presented for several cases of optimum and off-optimum circulations. The computation of the flowfields is based on the integral formulation of Ref. 3. The numerical procedures are those of Ref. 5. Several useful analytical expressions developed during the course of this research in connection with the computational approach are pre-

sented in Appendix A of this report. A generalized optimum performance theory applicable to rotors (or propellers) in axial motion is presented in Appendix B.

II. BACKGROUND

In recent years, the search for better methods of predicting rotor induced flowfield and associated performance in hover yielded a copious volume of literature on the subject. Several recent articles contain comprehensive bibliographies (Refs. 6 and 7) of the earlier work as well as review and reassessment of "classical" theories. The brief discussion given below provides a summary account of previous theories and present efforts. Only a few pertinent articles are referred to here. In many cases, a large number of articles exist which are based on essentially the same approach. Only one representative article is then mentioned.

As mentioned earlier, a hovering rotor is a special case of a propeller, with zero advance velocity. In the following discussion, however, the term "propeller" is used to describe only the case where the velocity of advance is of primary importance. The term "rotor" is used to describe the static propeller or the hovering rotor.

The majority of recent articles on rotor theory are concerned with the important problem of optimum performance. The central task in the performance study is the determination of a distribution of the rotor inflow velocity, over a given rotor disk, that leads to a minimum amount of power expenditure for a given amount of thrust. This information, when used in conjunction with the well known blade-element theory, permits the prediction of the performance limit and of the required radial distribution of circulation in order to approach this

limit. It thus provides a rational basis for blade design. The prediction of the optimum rotor performance, however, does not necessarily require a knowledge of the flowfield away from the rotor disk. In fact, the major portion of existing literature on rotor theory avoids the evaluating of the entire flowfield and treats the subject of optimum inflow velocity and optimum performance by themselves.

The earliest performance theory was the axial momentum theory based on the actuator disk (infinitely-bladed propeller) concept for propellers (Refs. 8 and 9). Within the context of this theory, the propeller operates without any frictional drag on the blade and induces no rotation in the slipstream. Since the flow upstream of the propeller disk is also irrotational, the tangential velocity component at the disk is zero. It follows from the Kutta-Joukowski theorem that the disk cannot be subjected to a lift force. Disregarding this inconsistency, two well known conclusions were obtained: first, an optimum propeller is one with a uniform axial velocity at the propeller disk, and second, when applied to a hovering rotor, the minimum power coefficient is equal to the thrust coefficient to the 3/2 power divided by the square root of 2. The theory provides no information on the radial distribution of circulation over the disk and consequently no indication as to how the blades should be designed for optimum performance.

In general, the energy loss due to the rotational motion in the slipstream of a propeller is small. The neglect of the slipstream rotation was therefore thought to be justified for the purpose of predicting the performance of propellers. The actual performance of propellers, however, generally does not meet the expectation of the axial

momentum theory even when the various loss factors, not including the slipstream rotation, are taken into account. This deficiency is explained by the general momentum theory, which incorporates a procedure to account for some of the effects of slipstream rotation. One of the major conclusions of the general momentum theory is that the slipstream rotation, though small in terms of the energy content, exerts an important influence on the optimum distribution of inflow velocity over the propeller disk. A detailed presentation of the general momentum theory is given in Ref. 10 which also contains a presentation of efforts directed toward the study of helicopter rotors. The general momentum theory does provide information on the optimum distribution of circulation over the disk. The solution as given in Ref. 10, however, is approximate and only partially accounts for the effects of slipstream rotation. Some of the neglected effects are of importance in the study of hovering rotors. For example, the conservation of angular momentum in the slipstream requires an exchange of energy between the rotational mode and the axial mode to accompany the contraction of the slipstream. The effect of this exchange of energy is neglected in the theory. For propellers where the velocity of advance is large compared to the induced velocity, the contraction is small and the neglect of the energy exchange is justified as long as the rotational energy is not excessively large. For hovering rotors, the ultimate wake cross-section is, to the first order, one half the size of the rotor disk. The exchange of energy therefore has a significant influence on the optimum distribution of circulation over the propeller disk for the situation where the rotational energy is not extremely small.

For rotor applications, it is therefore desirable to improve on the general momentum theory by fully accounting for the effects of slipstream rotation.

Until very recently, the theory which represents the current state of the art for routine calculation of propeller performance was the well-established vortex theory. The basic vortex theory represents the wake trailing the blades by a distribution of concentric cylindrical vortex sheets. These vortex sheets describe the radial variation of the blade circulation and thus imply an infinite number of blades. The effect of a finite number of blades is obtained approximately by Betz and Prandtl (Ref. 11) using a tip loss factor. An improved analysis by Goldstein (Ref. 12) represents the trailing vortex sheets in the ultimate wake, for optimum performance, by discrete helicoidal surfaces of constant helix angle and moving as rigid surfaces. Goldstein's work formed the basis of much of the subsequent analyses by Lock, Theodorsen, Lerbs, etc., (Refs. 13, 14, 15, 2 and 17) that proved to be sufficiently accurate for predicting propeller performance. The use of the vortex theory for predicting rotor performance, however, yielded overly optimistic results at high disk loadings (Ref. 1).

The continuing requirements of higher forward flight speed and larger rotorcraft, coupled with the need to keep the rotor small from weight and operational flexibility considerations, led to the development of rotors with higher rotational speed and disk loading. This resulted in increased inaccuracy of the vortex theory in predicting the rotor performance. Reviews of the vortex theory suggest that the wake contraction, the slipstream rotation, and the associated non-uniform

inflow are the factors that contribute most to the inability of the vortex theory to predict the hovering rotor performance accurately. This contention is supported by recent results obtained from the numerical computation of the entire rotor-induced flowfield.

In the numerical methods, typically, each rotor blade is represented by a lifting line with piecewise uniform circulation. The vorticity in the slipstream is represented by a number of discrete vortex filaments whose strengths are related to the discontinuities in circulation at the blades. Each vortex filaments is in turn approximately by a number of straight segments. If the geometry of the trailing vortex system is known, then the use of the Biot-Savart Law and the blade element theory yields a set of simultaneous equations. The solution of this set of equations gives the distribution of blade-bound vortex strength and hence also the trailing vortex filament strengths. The computations of velocities induced by the complete vortex system at all points in space, including those on the rotor disk, and of the thrust, the power, and the performance of the rotor are then straight forward.

For some rotor configurations and thrust levels, flow visualization studies have yielded useful wake geometry data. Methods that utilize experimentally obtained wake geometries in the numerical Biot-Savart Law approach described above are often referred to as the "prescribed-wake" analyses (Refs. 18, 19). For cases where experimental data permit the establishment of an accurate model for the wake geometry, the prescribed-wake analyses have yielded results in good agreement with experiments for overall performance (Ref. 7). For a general application

of the prescribed wake approach, however, accurate experimental data about the wake geometry must be available for a wide range of rotor configurations and thrust levels.

To remove the empiricism inherent in the prescribed wake approach, several researchers have developed methods which generate the wake geometry as a part of the computation procedure. This approach, sometimes referred to as the "free-wake" analysis (Ref. 20), employs an iterative or a time-step procedure to find, for a given rotor configuration, an arrangement of the vortex system which exists in "force-free equilibrium". The free-wake analysis generally incorporates a procedure to account for the convection of the vortex segments with the fluid but neglects the process of viscous diffusion. The analysis requires a relatively large amount of computer time for each combination of rotor configuration and thrust level. In order to determine rotor configurations that would give the optimum performance, a parametric study involving a large number of geometries must be studied. The amount of computer time required by the free-wake analyses in optimum performance studies is therefore extremely large. Also important is the fact that ·ually the free-wake analyses do not accurately predict the geometry of the wake in the region very near the rotor disk (Ref. 21) where the vortex system contributes greatly to the inflow velocity at the disk. For these reasons, the present utility of the free-wake analyses for design purposes is limited.

One advantage of the numerical Biot-Savart Law approach is that, in contrast to the previous theories which answer only the questions of performance, this approach provides information on the flowfield

surrounding the rotor as well. It must be recognized that the approach in use today is based on the inviscid flow analyses and its ability to accurately predict the rotor induced flowfield is subject to important limitations. In this regard, it is noted that a new numerical method which utilizes a generalized Biot-Savart Law and accounts for the process of viscous diffusion of vortices has been developed recently (Ref. 22). This method is applicable to the rotor problem.

In the inviscid numerical approach, each rotor blade is typically represented by a lifting line with piecewise uniform circulation. Thus, in addition to neglecting the viscous diffusion which tends to spread the vortex sheets into volume distributions of vorticity, the inviscid approach further lumps the surface distribution of vortices into vortex filaments for computational conveniences. A method formulated by T. Y. Wu (Ref. 3) for heavily loaded propellers, in contrast, utilizes the actuator disk concept and distributes the blade-bound vortex azimuthally over the propeller disk in an axi-symmetric manner. The trailing vortex sheets are now represented by a volume distribution of vortices in an axi-symmetric flow. The kinematics of the flow is formulated in terms of Stokes' stream function and the rotational velocity component. By the use of a Green's function, a non-linear integral equation for the stream function is established, allowing the solution for the stream function by successive approximations. The flowfield is thus formulated as a boundary value problem with a prescribed arbitrary radial distribution of circulation at the disk. The integral formulation of T. Y. Wu for the calculation of the stream function requires numerical quadrature of a triple integral containing a product of Bessel's functions

as the integrand. Two of the three ranges of integration are infinite. For these reasons the computational effort required, though less than the Biot-Savart Law approach, is still considerable.

Greenberg et al. (Refs. 4 and 5) utilized the integral formulation to compute flowfields induced by rotors with prescribed uniform and piecewise uniform circulation distributions. The Green's function in the integral formulation is recognized in their works as the stream function due to a circular vortex filament. By expressing the Green's function in terms of a Legendre function, the flowfield computations were accomplished reasonably rapidly. Similarly, Chaplin (Ref. 23) and Cox (Ref. 24) used the integral formulation in studies of axi-symmetric flows.

The actuator disk concept enjoys a substantial advantage in its relative simplicity. Results obtained on the basis of the actuator disk concept have been successfully used in the past as basic building blocks for the understanding of the practical problem of a rotor with a finite number of blades. For example, with the optimum distributions of circulation over infinitely-bladed rotor disks derived from the general momentum theory, the effect of a finite number of blades is obtained approximately by using Prandtl's formula (Ref. 11). Also, Greenberg and Kaskel's flowfield results for the infinitely-bladed rotor has been used by Erickson (Ref. 6) in a prescribed wake analysis. The research reported in the present work utilizes the simplicity offered by the actuator disk concept, but incorporates certain effects of slip-stream rotation which have been neglected in previous theories for rotor performance.

III. GENERAL FORMULATION

Consider a rotor hovering OGE in an incompressible and inviscid fluid. Following Prandtl's lifting line theory, each rotor blade is represented by a blade-bound vortex filament directed radially. If the strength of this vortex filament, i.e., the blade circulation, varies with the radial distance from the rotor axis, then there exists a vortex sheet trailing each blade. Within the context of the actuator disk concept, the total circulation of the several blades of the rotor is considered to be distributed uniformly over an infinite number of thin blades, each with a vanishingly small chord width. The discrete vortex sheets trailing the lifting lines (blades) are replaced by a volume distribution of vorticities within the slipstream. The problem is then time-independent and axi-symmetric about the rotor axis in a reference frame at rest relative to the fluid at infinity. That is, in a cylindrical coordinate system (r, θ, z) with the origin at the center of the disk and the z-axis coinciding with the rotor axis and pointing downstream, the flow parameters are all independent of the θ-coordinate and of the time t. The tangential, or θ-, component of the velocity vector, however, is not zero within the slipstream.

The general flow features for the hovering rotor OGE are shown in Fig. 1. For the present problem, the entire flow is induced by the rotor. Consequently the entire region outside of the slipstream and the blade row is "upstream" of the rotor.

The differential equations describing the flow are the familiar continuity and momentum equations:

$$\vec{\nabla} \cdot \vec{q} = 0 \tag{1}$$

and

$$(\vec{q} \cdot \vec{\nabla})\, \vec{q} = -\frac{1}{\rho} \vec{\nabla} p + \vec{F} \tag{2}$$

where $\vec{F}$ stands for the equivalent body force exerted on the fluid by the blade elements. The boundary conditions are that $\vec{q}$ vanishes infinitely upstream of the rotor and is independent of z infinitely downstream, i.e., in the ultimate wake.

For axi-symmetric flows, Eq. (1) can be rewritten as

$$\frac{1}{r} \frac{\partial}{\partial r} (ru) + \frac{\partial w}{\partial z} = 0 \tag{3}$$

where u and w are the radial and axial velocity components respectively. Therefore a Stokes' stream function $\psi(r, z)$ exists such that

$$u = -\frac{1}{r} \frac{\partial \psi}{\partial z} \tag{4}$$

and

$$w = \frac{1}{r} \frac{\partial \psi}{\partial r} \tag{5}$$

The flowfield is therefore completely determinate if ψ and the tangential velocity component v are known.

Introducing the vorticity vector $\vec{\omega}$ defined by

$$\vec{\omega} = \vec{\nabla} \times \vec{q} \tag{6}$$

one obtains the components of $\vec{\omega}$ in terms of ψ and v:

$$\xi = -\frac{\partial v}{\partial z} \tag{7}$$

$$\eta = -\frac{1}{r}\left(\frac{\partial^2 \psi}{\partial r^2} - \frac{1}{r}\frac{\partial \psi}{\partial r} + \frac{\partial^2 \psi}{\partial z^2}\right) \tag{8}$$

and

$$\zeta = \frac{1}{r}\frac{\partial}{\partial r}(rv) \tag{9}$$

The momentum equation can be rewritten in terms of $\vec{\omega}$ and the total head H as

$$\vec{q} \times \vec{\omega} = \vec{\nabla} H - \vec{F} \tag{10}$$

where

$$H = \frac{p}{\rho} + \frac{q^2}{2} \tag{11}$$

Outside the blade row, $\vec{F} = 0$ and therefore $\vec{q} \cdot \vec{\nabla} H = 0$ and $\vec{\omega} \cdot \vec{\nabla} H = 0$. Consequently, the gradient of H is perpendicular to both the velocity vector and the vorticity vector. In other words, the total head of the fluid is a constant along each stream tube except at the blade row where it may undergo an abrupt change. Upstream of the rotor, therefore, the total head is everywhere equal to the static pressure of the fluid far upstream divided by the density. Inside the slipstream, the total head is a function of the stream function only:

$$H = \frac{p_\infty}{\rho} \quad \text{upstream of the rotor} \tag{12}$$

$$= f(\psi) \quad \text{inside the slipstream}$$

Noting further that outside the blade row, since $\vec{F} = 0$ and the θ-component of $\vec{\nabla}H$ is zero because of axi-symmetry, one has

$$(\vec{q} \times \vec{\omega}) \cdot \vec{e}_\theta = 0$$

or

$$\vec{q} \cdot \vec{\nabla} (rv) = 0 \tag{13}$$

Consequently, outside the blade row, the gradient of rv is perpendicular to the velocity vector. In other words, the angular momentum of the fluid remains a constant along each stream tube except at the blade row where it may undergo an abrupt change. Since the angular momentum of the fluid is zero far upstream of the rotor, the angular momentum is zero everywhere outside the slipstream. Within the slipstream, the angular momentum is a function of the stream function only:

$$vr = 0 \quad \text{upstream of the rotor} \tag{14}$$

$$= g(\psi) \quad \text{inside the slipstream}$$

Consider the fluid passing the disk at $r = r_d$ as shown in Fig. 1. Equation (14) states that the tangential velocity component v of the fluid is zero on the upstream side of the disk and may be non-zero on the downstream side. Let v_d be the tangential velocity component of the fluid on the downstream side of the disk. There exists then a

discontinuity in v at the disk described by a distribution of radially directed vortices at the disk of strength v_d. The circulation of the blade-bound vortices at r_d is therefore $2\pi r_d v_d$. The tangential velocity at the disk is $\frac{1}{2}v_d$ in the principal value sense.

Within the context of the actuator disk concept, the blade-bound vortices are radially directed and axi-symmetrical. Therefore, the axial and radial velocity components of the fluid are both continuous at the disk. The continuity of the axial velocity at the disk is of course consistent with the law of conservation of mass.

Kutta-Joukowski theorem gives the lift (or thrust) and drag forces on the annular element of the disk $ds_d = 2\pi r_d dr_d$ as follows:

$$dT = \rho(\Omega r_d - v_d/2)\, v_d\, ds_d \tag{15}$$

$$dD = \rho\, w_d\, v_d\, ds_d \tag{16}$$

The rate of work done, or power expended, by the disk element ds_d is therefore

$$dP = \Omega r_d\, dD$$

$$= \rho\Omega\, w_d\, v_d\, r_d\, ds_d \tag{17}$$

The total thrust and total power of the rotor are obtainable by integrating Eqs. (15) and (17) respectively over the disk.

The mass flow rate through ds_d is $\rho w_d\, ds_d$. Therefore, from Eq. (17), one finds the increase in total head across the rotor disk to be $\Omega v_d\, r_d$. The total head on the downstream side of the disk is therefore

$$H_d = \frac{p_\infty}{\rho} + \Omega v_d r_d \tag{18}$$

According to Eqs. (12) and (14), H and vr are both functions of ψ only in the slipstream. One therefore has, from Eq. (18), in the slipstream

$$\frac{dH}{d\psi} = \Omega \frac{d}{d\psi}(vr) \tag{19}$$

The radial component of Eq. (10) gives

$$v\zeta - w\eta = \frac{\partial H}{\partial r} = \frac{dH}{d\psi}\frac{\partial \psi}{\partial r} \tag{20}$$

By using Eqs. (7), (9), (19), and (20), one obtains

$$\eta = -(\Omega r - v)\frac{d(vr)}{d\psi} \tag{21}$$

Consider now Eq. (8) which relates η to ψ. This equation is readily identified with the problem of circular vortices having the z-axis as a common axis. In many classical treatises on hydrodynamics (e.g., Ref. 25), the special case of an axi-symmetric rotational flow with v, ξ, and ζ all zero is discussed. The present problem is more general in that v, ξ and ζ are non-zero within the slipstream and, furthermore, $v(=\frac{1}{2}v_d)$ and ξ (blade-bound vortices) are non-zero at the rotor disk. The differential equations relating u, w, and η to ψ for the special case of zero v, ξ, and ζ, however, are identical to Eqs. (4), (5), and (8) derived for the general problem. This fact is not surprising since for the general axi-symmetric flow the continuity equation does not contain v and neither the radial vorticity distribution nor the axial vorticity distribution induces a velocity in a meridional

plane. As a consequence of this fact, certain kinematic relations between u, w, η and ψ available in the classical treatises for the special case of zero v, ξ, and ζ are directly applicable to the present, more general, problem. In particular, the differential equation (8) for ψ may be immediately recast into an integral representation for ψ:

$$\psi(r, z) = \iint_D G(r, z; r', z')\, \eta'\, dr'\, dz' \tag{22}$$

where the region of integration D covers the entire slipstream, G is the stream function at a field point (r, z) associated with a circular vortex filament with unit strength of radius r' and centers about the z axis in the plane z = z'. η' is the vorticity value in the slipstream at r', z'.

Several alternative forms of this Green's function are available in the literature (e.g., Ref. 25) and different authors developed different forms in their studies of the rotor and propeller problems. For example, an integral form involving Bessel functions of the first kind was utilized in Ref. 3 and a Legendre function of the second kind and the degree $\frac{1}{2}$ was utilized in Refs. 4 and 5. A convenient form to use is one involving complete elliptical integrals (Ref. 25, 26):

$$G = \frac{1}{2\pi} \sqrt{(r + r')^2 + (z - z')^2} \left\{ \left(1 - \frac{k^2}{2} \right) K(k) - E(k) \right\} \tag{23}$$

where

$$k = \left[\frac{4rr'}{(r + r')^2 + (z - z')^2} \right]^{\frac{1}{2}} \tag{24}$$

$$K(k) = \int_0^{\pi/2} \frac{1}{\sqrt{1 - k^2 \sin^2 \alpha}} \, d\alpha \tag{25}$$

$$E(k) = \int_0^{\pi/2} \sqrt{1 - k^2 \sin^2 \alpha} \, d\alpha \tag{26}$$

The functions K and E are complete elliptic integrals of the first and the second kind respectively. The properties and numerical values of these functions are readily available in mathematical handbooks.

The integral representation for ψ, Eq. (22) is a kinematic relation allowing ψ to be determined from any known distribution of η in the slipstream. It replaces the differential Eq. (8) together with certain boundary conditions. By putting Eq. (21) into Eq. (22), one obtains an integral representation equivalent to the ones derived by T. Y. Wu and by Greenberg, et. al. (Refs. 3, 4, and 5) using Green's functions. Greenberg et al. recognized the Green's function as the stream function due to a ring vortex. They subsequently used a vortex representation of the slipstream and developed an efficient method for computing the flowfields induced by the rotor.

During the course of the present investigation, several closed-form analytical solutions have been developed for the stream function and for velocities induced by several uniform and linear distributions of circular vortices over finite circular cylinders and annular surfaces. The solutions are expressed in terms of complete elliptic integrals and are presented in Appendix A of this report.

The availability of these analytical expressions contributes to the efficient and accurate computation of axi-symmetric flows.

IV. OPTIMUM PERFORMANCE THEORY

The Ultimate Wake

Consider the rotor hovering OGE. As shown in Fig. 1, the slipstream contracts downstream of the rotor and forms the ultimate wake far downstream where it no longer contracts. Thus, in the ultimate wake the radial velocity u vanishes and the flow is independent of the axial coordinate z. The fluid passing through the disk element ds_d passes through the annular element $ds_w = 2\pi r_w \, dr_w$ in the ultimate wake as shown in Fig. 1. By the law of mass conservation, one has

$$w_d \, ds_d = w_w \, ds_w \tag{27}$$

Equation (14) gives

$$v_d \, r_d = v_w \, r_w \tag{28}$$

The radial component of Eq. (2) gives in the ultimate wake

$$\frac{dp_w}{dr_w} = \frac{\rho v_w^2}{r_w} \tag{29}$$

This equation states simply that the centrifugal force of the fluid is balanced by the radial pressure gradient in the ultimate wake. Consider a spherical control volume of radius R centered at the origin of the coordinate system. The control surface consists of two parts S_1 and S_2, where S_1 is a cross section of the slipstream and S_2 is the remaining portion of the sphere. At large distances from the rotor disk, the

action of the rotor on the fluid outside the slipstream is equivalent to that of a sink, the strength of which is equal to the volume rate of flow passing through the disk, and is finite. Therefore, in the limit as $\mathcal{R} \to \infty$, $p = p_\infty + O(1/\mathcal{R}^4)$. Therefore the static pressure at the rim of the ultimate wake is p_∞. Equation (29) therefore gives

$$p_\infty - p_w = \rho \int_{r_w}^{R_w} \frac{v_w^2}{r}\, dr \tag{30}$$

Equation (12) requires $H_w = H_d$. It follows from Eqs. (14), (18), and (30) that

$$H_w = \frac{p_w}{\rho} + \Omega\, v_w\, r_w + \int_{r_w}^{R_w} \frac{v_w^2}{r}\, dr \tag{31}$$

However, in the ultimate wake, since $u_w = 0$, one has

$$H_w = \frac{p_w}{\rho} + \frac{v_w^2}{2} + \frac{w_w^2}{2} \tag{32}$$

Therefore

$$\frac{w_w^2}{2} = \Omega\, v_w\, r_w - \frac{v_w^2}{2} + \int_{r_w}^{R_w} \frac{v_w^2}{r}\, dr \tag{33}$$

At the rim of the ultimate wake,

$$\frac{w_{w_o}^2}{2} = \Omega\, v_{w_o}\, R_w - \frac{v_{w_o}^2}{2} \tag{34}$$

Consider again the control surface described earlier. The momentum theorem gives the following expression for the total thrust of the rotor

$$T = \int_{S_1} (p + \rho w^2)\, \vec{n} \cdot \vec{e}_z \, dS_1 + \int_{S_2} (p + \rho w^2)\, \vec{n} \cdot \vec{e}_z \, dS_2 \qquad (35)$$

where $\vec{n}$ is the unit outward normal vector on S_1 and S_2. As $R \to \infty$, the integrand in the second integral goes to $p_\infty + O(1/R^4)$. Therefore the second integral gives $-p_\infty(\pi R_w^2)$. Equation (35) therefore gives, with the use of Eq. (30) and Eq. (33),

$$T = \tfrac{1}{2}\rho \int_{S_1} \left[v_w(2\Omega r_w - v_w) + w_w^2 \right] ds_w \qquad (36)$$

The total power expended is, by using Eqs. (17), (27), and (28),

$$P = \rho\Omega \int_{S_1} w_w \, v_w \, r_w \, ds_w \qquad (37)$$

With a known radial distribution of the tangential velocity v_w in the ultimate wake, Eq. (33) establishes the distribution of w_w. Equations (36) and (37) then give the thrust and power of the rotor. A perturbation in the tangential velocity distribution therefore alters the thrust and the power. In the following section, a criterion for optimum performance is established by analyzing the changes in power and thrust resulting from the perturbation of the tangential velocity distribution. This criterion is first given in terms of the velocity distributions in the ultimate wake. These velocity distributions will subsequently be related to the optimum distribution of bound vorticity, thrust, and power.

Criterion for Optimum Performance

An optimum rotor is a rotor giving a specified amount of thrust while expending a minimum amount of power. Consider a given distribution of tangential velocity v_w in the ultimate wake. If a perturbation Δv_w in the tangential velocity is introduced as follows:

$$\Delta v_w = \begin{cases} 0 \quad , & \text{for } 0 < r_w < a \\ \epsilon r_w \, , & \text{for } a < r_w < a + \Delta r_w \\ 0 \quad , & \text{for } a + \Delta r_w < r_w < R_w \end{cases} \tag{38}$$

then, according to Eq. (33), the resulting change in the axial velocity distribution is

$$\Delta w_w = \begin{cases} 2v_{wa} \, \Delta r_w \, \epsilon / w_w \, , & \text{for } 0 < r_w < a \\ (\Omega a - v_{wa}) a \epsilon / w_w , & \text{for } a < r_w < a + \Delta r_w \\ 0 \, , & \text{for } a + \Delta r_w < r_w < R_w \end{cases} \tag{39}$$

where the subscript a indicates the value of v_w is evaluated at $r_w = a$. Only terms of the lowest order in $\epsilon a / v_{wa}$ and in $\Delta r_w / a$ are kept in each interval of interest.

Equations (36), (37), together with (38) and (39) gives the changes in thrust and power:

$$\Delta T = 2\pi\rho(\epsilon \Delta r_w) \, a^2 \, (2\Omega a - v_{wa}) \tag{40}$$

and

$$\Delta P = 2\pi\rho\Omega(\epsilon \Delta r_w) \, \{a^3 \, v_{wa}(\Omega a - v_{wa})/w_{wa}$$

$$+ a^3 w_{wa} + 2 v_{wa} \int_o^a \frac{v_w r_w^2}{w_w} dr_w \Big\} \qquad (41)$$

Equations (40) and (41) give

$$\Delta P = h(a)\ \Delta T \qquad (42)$$

where

$$h(a) = \frac{\Omega \left\{ a v_{wa} (\Omega a - v_{wa})/w_{wa} + a w_{wa} + \frac{2 v_{wa}}{a^2} \int_o^a \frac{v_w r_w^2}{w_w} dr_w \right\}}{2\Omega a - v_{wa}} \qquad (43)$$

is a function of a, the location where the perturbation of tangential velocity is introduced.

Suppose that a perturbation in tangential velocity is introduced at a_1 with resulting changes in power and thrust, ΔP_1 and ΔT_1. Suppose a second perturbation in tangential velocity is introduced at a_2 with resulting changes in power and thrust, ΔP_2 and ΔT_2. By suitably selecting the values of $\epsilon \Delta r_w$ at a_1 and a_2, the total change in thrust due to the two perturbations is made to vanish. Then $\Delta T_2 = - \Delta T_1$ and therefore

$$\Delta P = \Delta P_1 + \Delta P_2 = [h(a_1) - h(a_2)]\ \Delta T_1 \qquad (44)$$

Since ΔT_1 can be made either positive or negative by choosing the sign of ϵ in Eq. (40), it will be possible to obtain a negative value of ΔP if $h(a_1) \neq h(a_2)$. In other words, it is possible, by altering the tangential velocity distribution, to develop a given amount of thrust while expending a smaller amount of power. The tangential velocity distribution v_w under consideration therefore does not give optimum

performance.

It follows therefore that the optimum distribution of tangential velocity v_w is one which gives $h(a_1) = h(a_2)$. Since a_1 and a_2 are arbitrarily selected radial locations, the criterion for optimum performance is

$$h(r_w) = \text{constant} \tag{45}$$

In other words,

$$\int_o^{r_w} \frac{v_w}{w_w} r^2 dr = \frac{r_w^3}{2}\left[\frac{N}{r_w}\left(\frac{2\Omega r_w}{v_w} - 1\right) - \frac{w_w}{v_w} - \frac{\Omega r_w - v_w}{w_w}\right] \tag{46}$$

where N is a constant.

Computation Procedure

Equation (33) relates w_w to v_w. As a consequence, Eqs. (33) and (46) permit the evaluation of the optimum distribution of the tangential velocity v_w in the ultimate wake for specified values of N and R_w. Alternatively, Eqs. (33) and (46) are re-expressed in non-dimensional forms:

$$\frac{\tilde{w}_w^2}{2} = \tilde{v}_w \tilde{r}_w - \frac{\tilde{v}_w^2}{2} + \int_{\tilde{r}_w}^1 \frac{\tilde{v}_w^2}{\tilde{r}} d\tilde{r} \tag{47}$$

and

$$\int_o^{\tilde{r}_w} \frac{\tilde{v}_w}{\tilde{w}_w} \tilde{r}^2 d\tilde{r} = \frac{\tilde{r}_w^3}{2}\left[\frac{\tilde{N}}{\tilde{r}_w}\left(\frac{2\tilde{r}_w}{\tilde{v}_w} - 1\right) - \frac{\tilde{w}_w}{\tilde{v}_w} - \frac{\tilde{r}_w - \tilde{v}_w}{\tilde{w}_w}\right] \tag{48}$$

where

$$\tilde{v}_w = \frac{v_w}{\Omega R_w}$$

$$\tilde{w}_w = \frac{w_w}{\Omega R_w}$$

$$\tilde{r}_w = \frac{r_w}{R_w} \tag{49}$$

and $$\tilde{N} = \frac{N}{R_w}$$

From Eq. (47), one obtains at $\tilde{r}_w = 1$

$$\tilde{w}_{w_o} = [\,\tilde{v}_{w_o}(2 - \tilde{v}_{w_o})\,]^{\frac{1}{2}} \tag{50}$$

where the subscript "o" denotes the velocity components at the rim of the ultimate wake. Differentiating Eq. (47) with respect to r_w yields

$$\frac{d\tilde{w}_w}{d\tilde{r}_w} = (\tilde{r}_w - \tilde{v}_w)(\tilde{v}_w + \tilde{r}_w \frac{d\tilde{v}_w}{d\tilde{r}_w})/\tilde{r}_w \tilde{w}_w \tag{51}$$

From Eq. (48) and (50), one obtains at $r_w = 1$

$$\tilde{N} = \frac{(3 - 2\tilde{v}_{w_o})[\tilde{v}_{w_o}/(2 - \tilde{v}_{w_o})]^{\frac{1}{2}} + 2\tilde{v}_{w_o}\int_o^1 (\tilde{v}_w \tilde{r}^2/\tilde{w}_w)\, d\tilde{r}}{2 - \tilde{v}_{w_o}} \tag{52}$$

Differentiating Eq. (48) with respect to $\tilde{r}_w$ and using Eq. (51) yields

$$\frac{d\tilde{v}_w}{d\tilde{r}_w} = \frac{\tilde{v}_w\,[3\tilde{w}_w^4 - 2\tilde{N}(3\tilde{r}_w - \tilde{v}_w)\tilde{w}_w^3/\tilde{r}_w + \tilde{v}_w(5\tilde{r}_w - 2\tilde{v}_w)\tilde{w}_w^2 - \tilde{v}_w^2(\tilde{r}_w - \tilde{v}_w)^2]}{\tilde{r}_w[\tilde{w}_w^4 - 2\tilde{N}\tilde{w}_w^3 - \tilde{v}_w(\tilde{r}_w - 2\tilde{v}_w)\tilde{w}_w^2 + \tilde{v}_w^2(\tilde{r}_w - \tilde{v}_w)^2]} \tag{53}$$

If the value of $\tilde{v}_{w_o}$ is specified, then $\tilde{w}_{w_o}$ is determinate from Eq. (50). If, further, the value of $\tilde{N}$ is given, Equations (51) and (53) can be re-written as a system of two first order ordinary differential equations with "initial" values specified at the point $\tilde{r}_w = 1$, i.e., the rim of the ultimate wake. Various numerical methods are available for the solution of these equations. In the present work, a fourth order Runge-Kutta method is used to determine the distributions $\tilde{v}_w$ and $\tilde{w}_w$ from Equations (51) and (53) for specified values of $\tilde{v}_{w_o}$ and $\tilde{N}$. An iterative procedure is used with which a value of $\tilde{N}$ is estimated for the initial iteration. The distributions $\tilde{v}_w$ and $\tilde{w}_w$, obtained using this value of $\tilde{N}$ from Eqs. (51) and (53) are placed into Eq. (52) to compute a new value of $\tilde{N}$ for the second iteration. The iterations continue until the value of $\tilde{N}$ changes insignificantly between two successive iterations. In this manner, the optimum ultimate wake flow corresponding to a specified value of $\tilde{v}_{w_o}$ is established.

Contraction Ratio and Performance

The figure of merit of a rotor is defined by

$$M = \frac{1}{\sqrt{2}} \frac{C_T^{3/2}}{C_P} \tag{54}$$

where C_T and C_P are respectively the thrust coefficient and the power coefficient defined by

$$C_T = T/\pi\rho\Omega^2 R_d^4 \tag{55}$$

and

$$C_P = P/\pi\rho\Omega^3 R_d^5 \tag{56}$$

For a given radius of the ultimate wake, R_w, and a given angular velocity Ω of the rotor, the computed optimum distributions of $\tilde{v}_w$ and $\tilde{w}_w$ together with Eqs. (36) and (37) yield the corresponding thrust and power of the rotor. In order to establish the performance of the rotor, i.e., C_T, C_P and M, however, the disk radius R_d must be determined.

In theories of propeller performance, it is customary to write the thrust element in terms of the wake velocities as follows:

$$dT = \tfrac{1}{2}\rho[(2\Omega r_w - v_w)v_w + w_w^2]\, ds_w \tag{57}$$

The acceptance of Eq. (57) permits the radius of a given stream tube on the disk, r_d, to be related to the radius of that stream tube in the ultimate wake, r_w. Equating the right sides of Eqs. (15) and (57) and using Eq. (28) gives

$$\frac{dr_d}{dr_w} = \frac{[(2\Omega r_w - v_w)v_w + w_w^2]\, r_d}{(2\Omega r_d^2 - v_w r_w)v_w} \tag{58}$$

The boundary condition for this differential equation is

$$r_d = 0 \text{ at } r_w = 0 \tag{59}$$

With known distributions v_w and w_w, the quadrature of Eq. (58) gives r_d as a function of r_w and thus, for the given value of R_w, the value of R_d.

Equation (57) obviously satisfies Eq. (36). However, it is not the only expression that satisfies Eq. (36). Any function $b(r_w)$ which gives $\int_0^{R_w} b\,dr_w = 0$ can be added to the right side of Eq. (57) and the

resulting expression for dT still satisfies Eq. (36). It has been shown in Ref. 29, in fact, that no solution of Eq. (58) exists which satisfies the boundary condition (59). Accordingly, in the present research, an approach which does not utilize Eq. (58) is developed. In this approach, the contraction ration

$$c = r_w/r_d \tag{60}$$

is taken to be a constant independent of the radial location (r_w or r_d).

In general, the contraction ratio is a function of the radial location. The results of Ref. 2, however, indicate that no serious error is introduced by taking the contraction ratio to be a constant for heavily loaded free-running propellers. Thus it is expected that the assumption of constant contraction ratio is reasonable for the hovering rotor.

By taking c in Eq. (60) as a constant, Eqs. (15) and (28) yield

$$dT = \rho \left(\frac{\Omega r_w}{c^2} - \frac{v_w}{2} \right) v_w \, ds_w \tag{61}$$

Integrating Eq. (61) and equating the right side of the resulting equation to the right side of Eq. (36) gives, after rearrangement of terms,

$$c = \left[1 + \frac{\int_0^{R_w} w_w^2 \, ds_w}{2\Omega \int_0^{R_w} v_w \, r_w \, ds_w} \right]^{-\frac{1}{2}} \tag{62}$$

Noting that, using integration by parts,

$$\int_0^{R_w} w_w^2 \, r_w \, dr_w = \frac{w_{w_o}^2 R_w^2}{2} - \tfrac{1}{2} \int_0^{R_w} \frac{dw_w^2}{dr_w} r_w^2 \, dr_w \tag{63}$$

Differentiating Eq. (33) gives

$$\tfrac{1}{2} \frac{dw_w^2}{dr_w} = \Omega v_w + \Omega r_w \frac{dv_w}{dr_w} - \tfrac{1}{2} \frac{dv_w^2}{dr_w} - \frac{v_w^2}{r_w} \tag{64}$$

Placing Eq. (64) into (63) and noting that

$$\int_0^{R_w} \frac{dv_w}{dr_w} r_w^3 \, dr_w = v_w R_w^3 - 3 \int_0^{R_w} v_w \, r_w^2 \, dr_w \tag{65}$$

and

$$\int_0^{R_w} \frac{dv_w^2}{dr_w} r_w^2 \, dr_w = v_w^2 R_w^2 - 2 \int_0^{R_w} v_w^2 \, r_w \, dr_w \tag{66}$$

One then has

$$\int_0^{R_w} w_w^2 r_w dr_w = \frac{w_{w_o}^2 R_w}{2} - \Omega v_w R_w^3 + \tfrac{1}{2} v_w^2 R_w^2 + 2\Omega \int_0^{R_w} v_w r_w^2 dr_w \tag{67}$$

Using Eq. (34) then gives

$$\int_0^{R_w} w_w^2 \, r_w \, dr_w = 2 \Omega \int_0^{R_w} v_w \, r_w^2 \, dr_w \tag{68}$$

Consequently, Eq. (62) becomes

$$c = \frac{R_w}{R_d} = \frac{1}{\sqrt{2}} \tag{69}$$

It is noted that this contraction ratio is precisely the value predicted by the axial momentum theorem.

With c known, R_d immediately follows from the specified value of R_w ($R_d = \sqrt{2}\, R_w$). The axial inflow velocity and the circulation at the rotor disk are related to the axial and tangential velocities in the ultimate wake. The thrust and power coefficients as well as the figure of merit can be easily evaluated from the known flow conditions in the ultimate wake. In particular, once an optimum distribution of v_w is established, the corresponding distribution of w_w, w_d, and P, the values of C_T, C_P, and M immediately follow.

The optimum rotor performance theory described here has been generalized to the case of a rotor (or a propeller) in axial motion. The analysis for this general case is presented in Appendix B of this report.

7. ROTOR INDUCED FLOWFIELD

A number of methods have been developed by various authors for the solution of Eqs. (21) and (22), with specified distribution of disk-bound circulation (Refs. 3, 4, 5, 23, 24). The approach chosen for the present work is the numerical method described by Greenberg et al. (Refs. 4 and 5).

For the hovering rotor problem, the domain of integration in Eq. (22) is the entire slipstream and is not known a priori. In fact, the shape of the stream tubes bounding and within the slipstream is to be established as a part of the solution. Following the approach of Greenberg and Powers (Ref. 5), the specified distribution of circulation at the disk is approximated by a piecewise uniform distribution as shown in solid lines in Fig. 2. The disk radius is divided into L segments at radii $r_d = R_o, R_1, \ldots R_L$, with $R_o = 0$, and $R_L = R_d$. In the ℓ th segment, $R_{\ell-1} < r_d < R_\ell$, the circulation is taken to be a constant value Γ_ℓ. The trailing vortices are considered to be shed only at the radial locations R_ℓ. The slipstream vortex system is then represented by L discrete vortex tubes. The ℓth vortex trails the disk at $r_d = r_\ell$. Equation (22) becomes

$$\psi(r, z) = \sum_{\ell=1}^{L} \int_o^\infty G(r, z; t_\ell', z')\, \gamma_\ell'\, dz' \qquad (70)$$

where t_ℓ is the radius of the ℓth vortex tube and γ_ℓ' is the strength of the ℓth vortex tube. t_ℓ' and γ_ℓ' are both functions of z'.

With the above representation of the slipstream vortex system, the vorticity in the regions between the vortex tubes is zero. The angular momentum vr of the fluid is constant between the vortex tubes and changes discontinuously across the tubes by the amount $(\Gamma_{\ell+1} - \Gamma_\ell)/2\pi$. Consider for the moment a continuous, though rapid, change of the angular momentum in the interval $r = t_\ell$ to $r = t_\ell + \Delta r$. The corresponding volume distribution of the tangential vorticity η_ℓ is given by Eq. (21), i.e.

$$\eta_\ell = - (\Omega r - v) \frac{d(vr)}{d\psi} \tag{71}$$

As Δr approaches zero, one obtains a vortex tube with strength

$$\gamma_\ell = \eta_\ell \, \Delta r = - \left[r(\Omega - \frac{vr}{r^2}) \frac{d(vr)}{d\psi} \Delta r \right]_{r = t_\ell} \tag{72}$$

The angular momentum vr at $r = t_\ell$ is, in the principal value sense, equal to $\frac{1}{2}\left[(vr)_\ell + (vr)_{\ell+1} \right]$, or equivalently $(\Gamma_\ell + \Gamma_{\ell+1})/4\pi$. Thus Eq. (72) may be re-written as

$$\gamma_\ell = - \left[\Omega - \frac{1}{4\pi t_\ell^2} \left(\Gamma_\ell + \Gamma_{\ell+1} \right) \right] \left(\frac{\Gamma_{\ell+1} - \Gamma_\ell}{2\pi} \right) \left(r \frac{dr}{d\psi} \right)_{r=t_\ell} \tag{73}$$

Using Eq. (5), one then obtains

$$\gamma_\ell \, w_\ell = \frac{\Gamma_\ell - \Gamma_{\ell+1}}{2\pi} \left[\Omega - \frac{1}{4\pi t_\ell^2} \left(\Gamma_\ell + \Gamma_{\ell+1} \right) \right] \tag{74}$$

where w_ℓ is the axial velocity on the ℓth vortex tube in the principal

value sense.

Equation (74) has been derived in Ref. 5 using the Bernoulli's equation and the condition that the vorticity in the slipstream convects with the fluid motion. The present, alternative, derivation of this equation points out that, instead of considering the trailing vortex tubes to originate at the disk radii R_ℓ, it would also be appropriate to lump the vortices shed within each interval $R_{\ell-1} < r_d < R_\ell$ into a vortex tube originating at the mid-point of that interval, i.e., at $r_d = \frac{1}{2}(R_{\ell-1} + R_\ell)$. This mid-point representation is shown in dashed lines in Fig. 2. While the end-point representation used in Ref. 5 describes the disk bound circulation well, it appears that the mid-point representation would describe the slipstream vortex system more accurately. With the mid-point representation, if the circulation goes to zero continuously at $r_d = R_d$, then the slipstream boundary is no longer identified by the outermost vortex tube. For this situation, the mid-point representation must be modified for the outermost interval if the slipstream boundary is to be identified. The mid-point representation also presents some difficulties for the innermost interval. In Ref. 5, attempts were made to provide a cut-out, i.e., to let $\Gamma_1 = 0$, representing the finite hub of the rotor. These attempts failed to produce convergent results. The use of the mid-point representation for the innermost interval is computationally equivalent to the use of an end-point representation and assign $\Gamma_1 = 0$ for the interval $0 \le r_d \le R_1/2$. Thus it is expected that the use of the mid-point representation for the innermost interval would also present convergence problems.

A possible method of removing the above noted difficulties is to use continuous distributions of blade-bound vortices, or circulation, for the innermost and the outermost intervals. It should be noted that in Refs. 4 and 5, it was pointed out that with the end point representation, the strength of the outermost vortex tube becomes singular at the tip of the slipstream. Furthermore, if the circulation for the innermost interval is non-zero, then the tangential velocity v becomes infinitely large at r = 0 and the rotor's thrust diverges. Therefore there existed also difficulties in using end-point representations for the innermost and outermost intervals. Again, a possible method of removing these difficulties is to use continuous distributions of blade-bound vortices for the innermost and outermost intervals. Inasmuch as satisfactory results were obtained by the use of the method described in Ref. 5 for the major portion of the flowfield of concern, no attempt has been made to incorporate the "continuous" representation of blade-bound vortices.

Since the vortex tubes in the slipstream coincide with the stream tubes, the application of Eq. (70) at each vortex tube m gives

$$\psi_m = \sum_{\ell=1}^{L} \int_o^\infty G(t_m, z; t_\ell;, z')\, \gamma'\, dz' \qquad (75)$$

where ψ_m is a constant. Equations (5), (70) and (74) give

$$\sum_{\ell=1}^{L} \int_o^\infty G_r(t_m, z; t_\ell', z')\, \gamma_\ell'\, dz' = \frac{t_m (\Gamma_m - \Gamma_{m+1})}{2\pi\, \gamma_m} \left[\Omega - \frac{1}{4\pi t_m^2} (\Gamma_m + \Gamma_{m+1}) \right] \qquad (76)$$

where

$$G_r(r, z; r', z') = -\frac{1}{2\pi r' \sqrt{(z'-z)^2 + (r'+r)^2}} \left\{ K(k) \right.$$

$$\left. - \left[1 + \frac{2r(r-r')}{(z'-z)^2 + (r'+r)^2} \right] E(k) \right\} \qquad (77)$$

Equations (75) and (76) constitute a set of 2L coupled integral equations containing the 2L unknown functions $t_i(z)$ and $\gamma_i(z)$. An iterative method of solution of this set of integral equations is described in Ref. 5.

VI. RESULTS AND DISCUSSION

Optimum Performance

a. Optimum Circulation Distribution

Numerical results for the optimum radial distribution of circulation and inflow velocities at the rotor disk and the associated performance parameters have been obtained for 16 values of the thrust coefficient between 0.001 and 0.050. This range of thrust coefficient was considered to bracket the normal operating range of hovering rotors. In Ref. 27, the optimum radial distributions of the circulation and of the axial inflow velocity at the disk are presented for the 16 values of the thrust coefficient. It is noted in Ref. 27 that for small values of the thrust coefficient, the optimum circulation and the axial inflow velocity are nearly independent of the radial position except near the axis. For higher values of the thrust coefficient, the deviations of the optimum circulation and of the axial inflow velocity from constant values extend over larger regions and the magnitude of the deviations are larger.

The optimum distribution of circulation is presented for the thrust coefficients of 0.001, 0.005, 0.010, and 0.050 in Fig. 3. In Ref. 10, an approximate solution for the hovering rotor problem is given based on the general momentum theory neglecting the radial pressure gradient in the umtimate wake. The approximate distributions of circulation of Ref. 10 are computed and compared with the present, more exact, solution in Figure 3. The comparison shows that

the approximate solution of Ref. 10 deviates significantly from the present result, particularly in the inboard region of the disk. The deviations are more severe for larger values of the thrust coefficient.

b. Axial Inflow Velocity

In Fig. 4, the optimum distributions of axial inflow velocity obtained in the present study are presented and compared with the approximate solution of Ref. 10 for several values of C_T. It is noted that the approximate solution of Ref. 10 gives a zero value of the axial inflow velocity at the axis of the disk. It has been shown in Refs. 27 and 29 that this zero axial inflow velocity is incorrect.

c. Figure of Merit

Insofar as the overall performance of the rotor is concerned, the approximate method of Ref. 10 yields a figure of merit more optimistic than the more exact results of the present theory. Figure 5 shows that the computed figure of merit based on the present theory is lower than that based on the approximate theory of Ref. 10, which is in turn much lower than the ideal figure of merit of one. The deviations between the results increases with the value of the thrust coefficient.

d. Effect of Finite Number of Blades

While the present investigation is primarily concerned with an infinitely bladed rotor, the effect of a finite number of blades may be determined, for example, by extending Lerbs' work (Ref. 17) on heavily loaded, free running propellers.

An estimate of the effect of number of blades on the optimum distribution of circulation is provided by modifying Prandtl's approxi-

mate method (Ref. 11) of calculating the "tip loss" factor and applying the result to the hovering rotor case. The procedure is outlined in Ref. 27. The results are shown in Figure 6 for rotors with 2, 4, and 6 blades at $C_T = 0.010$. Based on these results, the corrected thrust coefficients for 2, 4, and 6 blades are respectively 0.00759, 0.00865, and .00906. The corresponding corrected power coefficients are .000547, 0.000624, and 0.000655. The figures of merit are 0.855, 0.911, and 0.931. In comparison, without the tip loss correction, the power coefficients for the infinitely bladed rotor are respectively (at $C_T = 0.00759$, 0.00865, and 0.00906) 0.000479, 0.000585, and 0.000627. The figures of merits are 0.975, 0.973, and 0.972.

Rotor Induced Flow

Following the analyses described in the previous sections, a computer program was prepared to compute the flowfields associated with the optimum distribution of circulation. In these computations, emphasis was placed on the determination of the shapes of the stream tubes in the slipstream. As discussed earlier, the vortex tubes coincide with the stream tubes in the slipstream.

The continuous circulation distribution was represented by a number of piecewise uniform circulation intervals and the trailing vortex tubes are considered to originate from the end-points of each interval as was done in Ref. 5. The value of the circulation within the ℓth interval was taken to be

$$\Gamma_\ell = \frac{2\pi}{\Omega(R_\ell^2 - R_{\ell-1})^2} \int_{r_{\ell-1}}^{r_\ell} (2\Omega r_d - v_d)\, v_d\, r_d dr_d \qquad (78)$$

It shall be shown later that the thrust developed in the ℓth interval due to the constant circulation Γ_ℓ given by Eq. (78) is approximately equal to that due to the continuous distribution of circulation $\Gamma_\ell = 2\pi v_d r_d$.

a. Effects of Number of Intervals Used

Three sets of computations were made for the case of an optimum rotor hovering OGE with a thrust coefficient of 0.010 using 4, 5, and 7 constant circulation intervals. For the set of computations using 4 intervals, the values of R_ℓ's were assigned to be 0.00 R, 0.15 R, 0.30 R, 0.60 R, and 1.00 R. For the 5- interval computations, additional R_ℓ values were assigned at 0.80 R. For the 7-interval computations, additional R_ℓ values were assigned at 0.45 R, 0.75 R, and 0.90 R. A comparison of the computed stream tube shapes based on 4-, 5-, and 7-interval representations is shown in Fig. 7. The comparison revealed that the three sets of computations gave practically identical stream tube shapes. The maximum deviations in the computed radius of the slipstream boundary was less than 0.2% between the three sets of results. A similar comparison of the axial inflow velocities revealed that, except in the immediate vicinity of the additional R_ℓ's, the results are virtually independent of the number of intervals used. These comparisons suggest that a 4- or 5- interval representation is adequate for routine computations.

b. Effects of Second Order Terms

According to Eq. (15), if Γ_ℓ is such that the thrust developed in the ℓth interval due to Γ_ℓ is equal to that due to the continuous distribution of circulation $\Gamma = 2\pi v_d r_d$, then

$$\Omega(R_\ell^2 - R_{\ell-1}^2)\,\Gamma_\ell - \frac{1}{2\pi}\ln\left(\frac{R_\ell}{R_{\ell-1}}\right)\Gamma_\ell^2$$

$$= 2\pi\int_{R_{\ell-1}}^{R_\ell} (2\Omega\, r_d - v_d)\, v_d\, r_d\, dr_d \qquad (79)$$

The second term on the left side of Eq. (79) represents a second order effect of the slipstream rotation. If this term is neglected, then one obtains the expression for Γ_ℓ given by Eq. (78). In general, the maximum value of Γ_ℓ is approximately equal to $2\pi\Omega R_d^2 C_T$. For usual applications, since C_T is much smaller than unity, the second term on the left side of Eq. (79) is negligible for all intervals $\ell \neq 1$. For the first interval, $\ell = 1$, one has $R_{\ell-1} = R_o = 0$ and the second term becomes infinitely large. Thus, Eq. (79) is not appropriate for the first interval. It should be noted that in reality, the area represented by the first interval is equal to πR_1^2 and is a small fraction of the total disk area πR_L^2. For example, by taking $R_1 = 0.15\ R_L$, the area represented by the first interval is 2.25% of the total disk area. Since the value of the circulation in the first interval is also small, the thrust developed in the first interval is only a small fraction of the total rotor thrust. The piecewise constant circulation Γ_ℓ as determined by Eq. (78) therefore gives a total rotor thrust very nearly equal to the total rotor thrust due to the continuous circulation distribution $\Gamma = 2\pi\, v_d\, r_d$.

The second term inside the brackets in Eq. (74) also represents a second order effect of the slipstream rotation. This term again is negligible for all except the innermost interval. In this investigation,

the role of this second order term in defining the vortex tube shapes is examined by computing, for the $C_T = 0.01$ case using 7-intervals, the vortex tube shapes neglecting and accounting for this second-order effect. The results, shown in Figure 8, indicate that the neglect of this second-order effect leads to a slightly smaller ultimate wake. The effect is small for all except the innermost streamtube.

c. Restriction on the Radius of the Innermost Tube

Equation (79) shows that if as $r_d \to 0$, the continuous distribution of circulation, Γ, goes to zero as r^α, with $\alpha > 0$, then the thrust developed in the first interval is finite. If the continuous distribution of circulation is replaced by a constant, non-zero, circulation in the first interval, then as $r_d \to 0$ the tangential velocity component goes to infinity as $1/r_d$ and the thrust becomes infinitely large. Greenberg et. al. made several attempts (Ref. 5) to remove this difficulty by letting $\Gamma_1 = 0$. They pointed out that this is equivalent to providing a cut-out to represent a finite hub of the rotor. These attempts, however, failed to produce any convergence solution. In the present investigation, it was observed that the convergence of the numerical solution was also sensitive to the value of R_1 used in the computation procedure. Convergence was not obtained with $R_1 = 0.10$. However, with $R_1 = 0.15$, convergence was obtained. The difficulties experienced is attributable to the fact that the innermost vortex tube was situated in an essentially dead-air or recirculating flow region, as can be shown by examining the axial velocity in the ultimate wake.

Since the vorticity between two adjacent vortex tubes is zero and since the radial velocity is zero in the ultimate wake, the axial

velocity in the ultimate wake is constant between two vortex tubes. Let W_ℓ be the constant ultimate axial velocity in the ℓth interval (i.e., between the $(\ell-1)$th and the ℓth vortex tubes), then, in the ultimate wake

$$\gamma_\ell = W_\ell - W_{\ell+1} \tag{80}$$

$$w_\ell = \tfrac{1}{2}\,(W_\ell + W_{\ell+1}) \tag{81}$$

Applying Eq. (74) in the ultimate wake then yields

$$W_\ell^2 = W_{\ell+1}^2 + \frac{\Omega}{\pi}\,(\Gamma_\ell - \Gamma_{\ell+1}) - \frac{1}{4\pi^2 t_\ell^2}\,(\Gamma_\ell^2 - \Gamma_{\ell+1}^2) \tag{82}$$

Noting that the axial velocity and the circulation is zero outside the ultimate wake and neglecting the second order terms in Eq. (82) gives

$$W_\ell^2 = \frac{\Omega}{\pi}\,\Gamma_\ell$$

and in particular

$$W_1^2 = \frac{\Omega}{\pi}\,\Gamma_1$$

Consequently, if one lets $\Gamma_1 = 0$ as was attempted in Ref. 5, then $W_1 = 0$ and the net flow passing within the innermost stream tube is zero. Thus the innermost vortex tube contains a dead-air or recirculating flow region. Such regions obviously are not amenable to the iterative proceedure used here.

It can be shown that the inclusion of the second order terms in

Eq. (82) increases the values of W. Therefore, W_1 is non-zero even if one lets $\Gamma_1 = 0$. This non-zero value of W_1, however, is small and the innermost stream tube still contains essentially a dead-air region. Similarly, since the continuous distribution of circulation approaches zero near the axis of the rotor, the value of Γ_1 is small if the value of R_1 is small. As a result, W_1 becomes very small and the innermost stream tube again contains essentially a dead-air region. These observations were substantiated by the numerical results obtained in this investigation.

d. Stream Tube Shapes

In addition to the case of $C_T = 0.010$, computations were made for the previously discussed optimum distributions of circulations at $C_T = 0.001, 0.005, 0.050$. For these additional computations, the 4-interval representation was used. The computed slipstream shapes are presented in Figs. 9 for cases of 0.001, 0.010, and 0.050. The shape for the case of $C_T = 0.005$ lies between those for $C_T = 0.001$ and 0.010 and is not shown. The results show that with increasing values of C_T, the "dead-air" region near the hub becomes more prominent. The contraction ratio is nearly independent of the radial location. For the cases studied, this ratio deviated from the universal value of 0.742 by less than one half of a percent. This value is somewhat larger than the value 0.707 predicted by the momentum theory. The computed axial velocity in the ultimate wake, also shown in Figs. 9, for $C_T = 0.010$, is in good agreement with that predicted by Eq. (82). Furthermore, for the smaller values of C_T, the computed axial velocity is in good agreement with the optimum ultimate wake velocity. For the case of $C_T = 0.050$, however,

the computed axial velocity is significantly lower than the optimum wake velocity near the axis of the rotor.

In addition to the optimum circulation distribution cases, computations were made using the circulation distribution given in Fig. 6 for the two-bladed rotor with tip-loss correction. This special distribution of circulation shall be referred to as off-optimum circulation since the present computation procedure is specifically designed for infinitely bladed rotors.

The slipstream geometry for the off-optimum circulation case is compared with the optimum circulation case of $C_T = 0.010$ in Fig. 10. The comparison shows that the ultimate wake radius is smaller for the off-optimum case than for the optimum case.

The slipstream boundary shapes for a rotor with constant circulation hovering in ground effect at heights R_d and $2R_d$ above the ground plane are computed and shown in Fig. 11. Also shown in Fig. 11 are the experimental results of Ref. 18 obtained from smoke pictures for a two-bladed rotor hovering at a height of R_d above the ground plane. It appears that, within the limitations of the infinitely bladed model for the rotor, the computed results provide a reasonable description of the wake boundary. Computations were also made for a rotor hovering at a height 10 R_d above the ground plane. It was found for this case, the flowfield at distances $3R_d$ or more above the ground plane is nearly identical to that of a rotor hovering OGE.

VII. CONCLUSIONS

Studies of the optimum performance and of the induced potential flowfields of rotors and propellers are made on the basis of a "rotating actuator disk" concept. By modifying and adopting certain principles and techniques of propeller aerodynamics, a new criterion for the optimum performance of rotors and propellers in axial flight is obtained. The analysis leading to this criterion is more complete than the previous analyses in that the present analysis fully accounts for the effects of slipstream rotation and allows for the existence of a radial pressure gradient in the ultimate wake. For flowfield computations, the radial distribution of circulation at the rotor disk is represented by a piecewise uniform distribution of circulation. The slipstream is represented by a set of axi-symmetric vortex tubes shed from the disk at the locations of circulation discontinuities. Existing numerical methods are utilized to compute the shape and strength of the vortex tubes that satisfy the required kinetic and kinematic conditions for the slipstream. Numerical results are obtained for hovering rotors (static propellers) in and out of ground effect for cases of optimum and off-optimum circulation distributions at various thrust levels.

Several conclusions of the present study are summarized below:

1. Previous investigators comparing experimental data with theoretical results noted that the earlier theories, in which the effect of slipstream rotation is partly or totally neglected, generally overestimate the optimum performance of hovering rotors in the higher thrust

coefficient range of practical interest. The present theory provides improvements in theoretical predictions by fully accounting for the effects of slipstream rotation. These improvements, which are not important in the case of a lightly loaded propeller, have significant influence on the optimum distribution of blade-bound circulation and hence power and thrust requirements of hovering rotors. The inaccuracies of the earlier theoretical results that are attributable to the neglected slipstream rotation effects increase with increasing thrust coefficient. Thus the improvements of the present theory are particularly important in the higher thrust coefficient range.

2. The rotating actuator disk concept permits the calculation, in a straightforward manner, of the optimum distribution of circulation and inflow velocity over the rotor disk for the infinitely bladed case. The potential flowfield induced by the infinitely bladed rotor and the effect of finite blade number on the circulation distribution are estimated, by using available methods, for the optimum circulation distributions.

3. In the flowfield computation, the continuous circulation distribution was represented by a number of piecewise uniform circulation intervals. The computed results show that representation of the continuous circulation distribution by as few as four piecewise uniform intervals is adequate for routine computations of the slipstream and of the streamtubes within it.

4. The computed slipstream shapes for rotors hovering OGE show that the dead-air region near the hub becomes more prominent with increasing value of the thrust coefficient. The slipstream contraction ratio is

nearly independent of the radial location and of the thrust coefficient. The computed value of the contraction ratio is somewhat larger than the value of 0.707 predicted by the axial momentum theory.

5. Computations for rotors hovering in ground effect show that within the limitations of the infinitely bladed model, the computed results provide a reasonable description of the wake boundary. For a rotor hovering at a height of ten rotor radii above the ground plane, the flowfield above about 3 radii distance from the ground plane is nearly identical to that of a rotor hovering OGE.

6. A number of explicit formulae useful in computing rotor and propeller induced flows are made available for the stream function and velocities due to distributions of circular vortices over axi-symmetric surfaces.

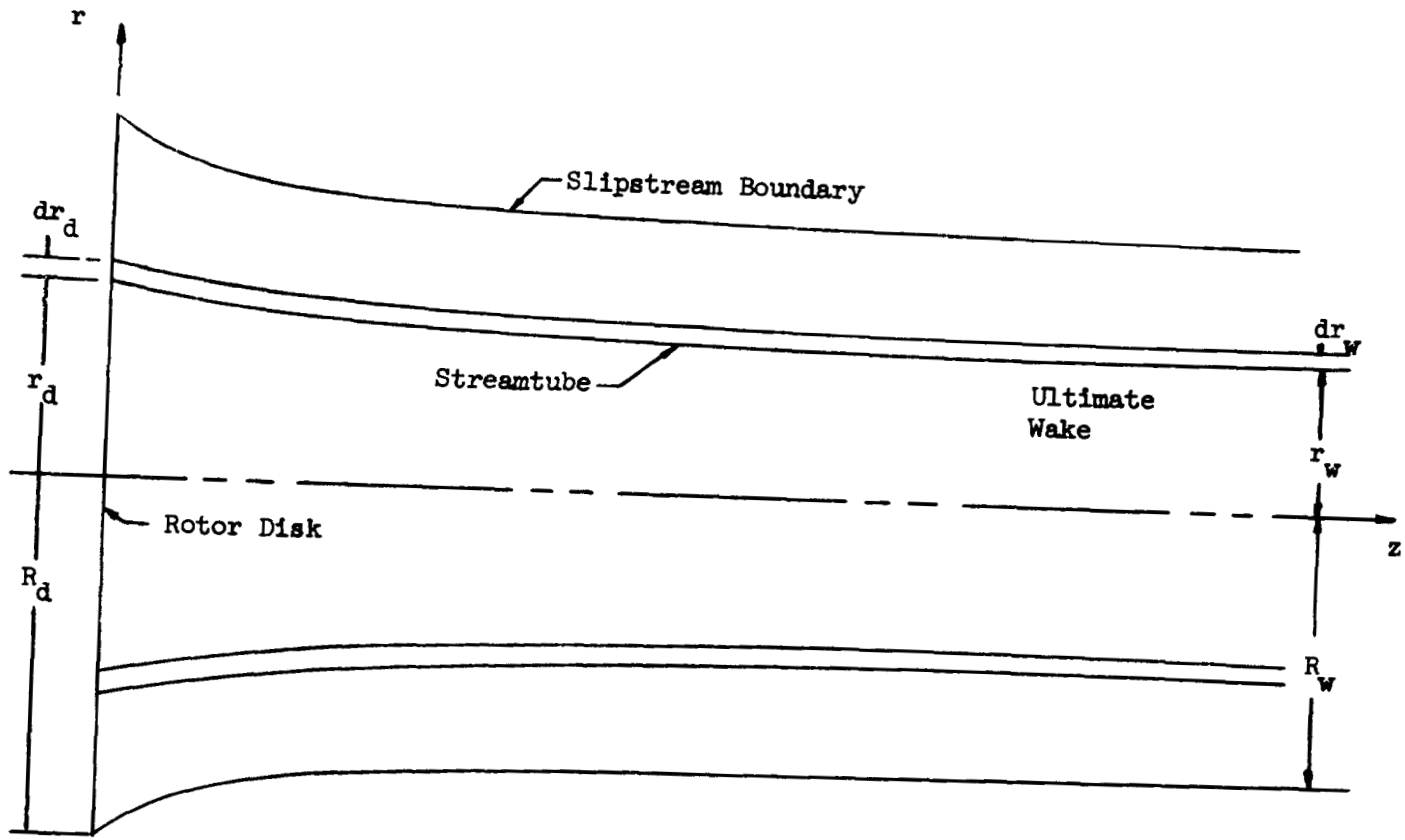

Figure 1. Flow Geometry

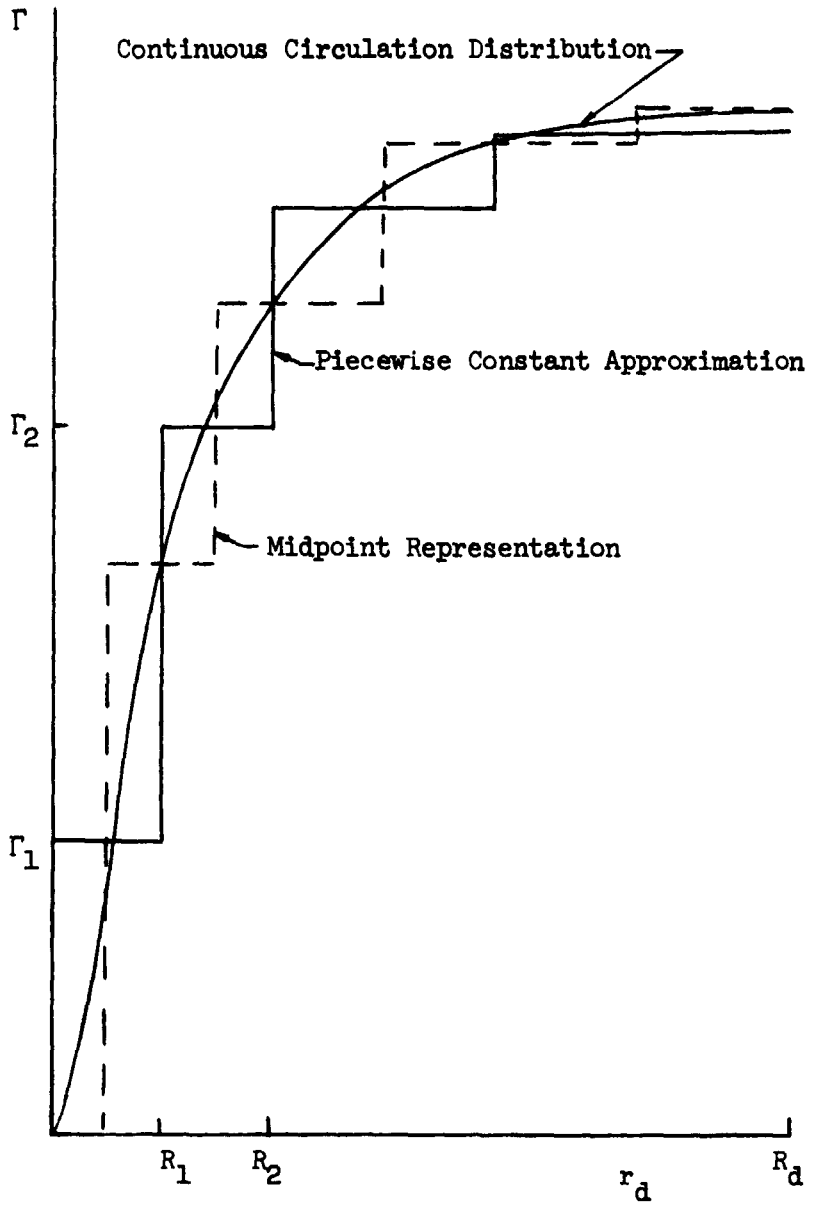

Figure 2. Piecewise Constant Approximation of Circulation at the Disk

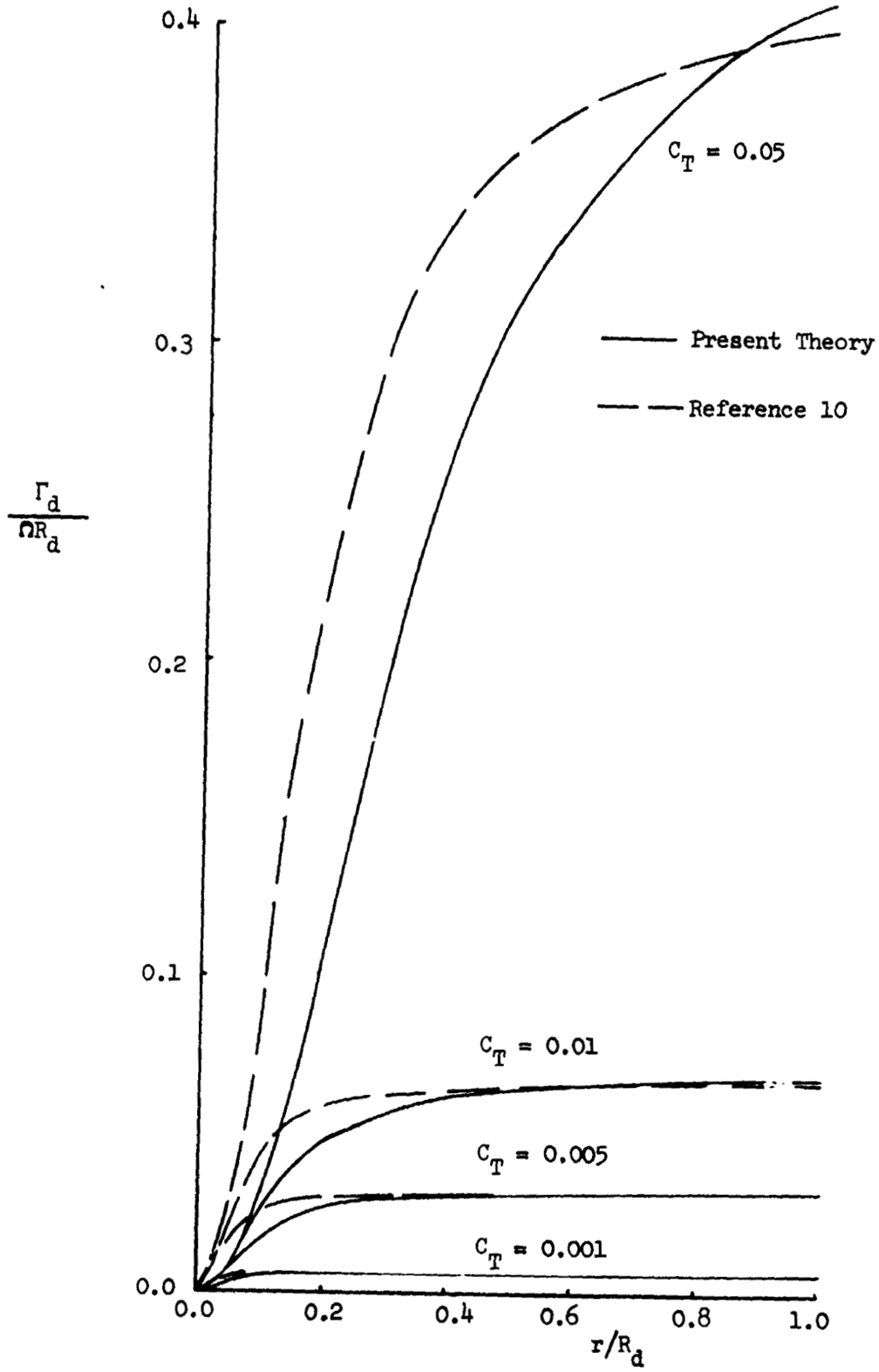

Figure 3. Optimum Radial Distributions of Circulation

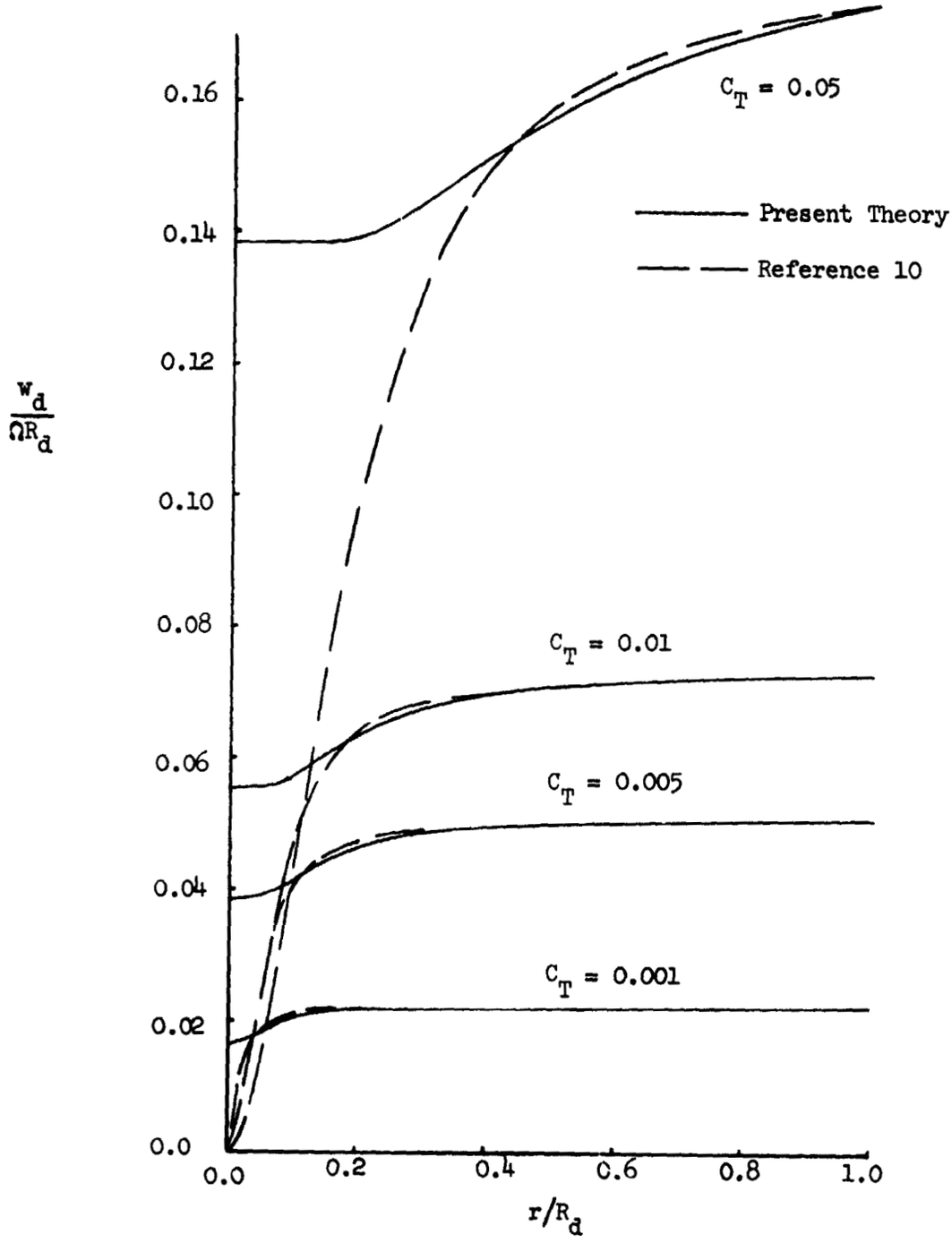

Figure 4. Optimum Radial Distribution of Axial Inflow

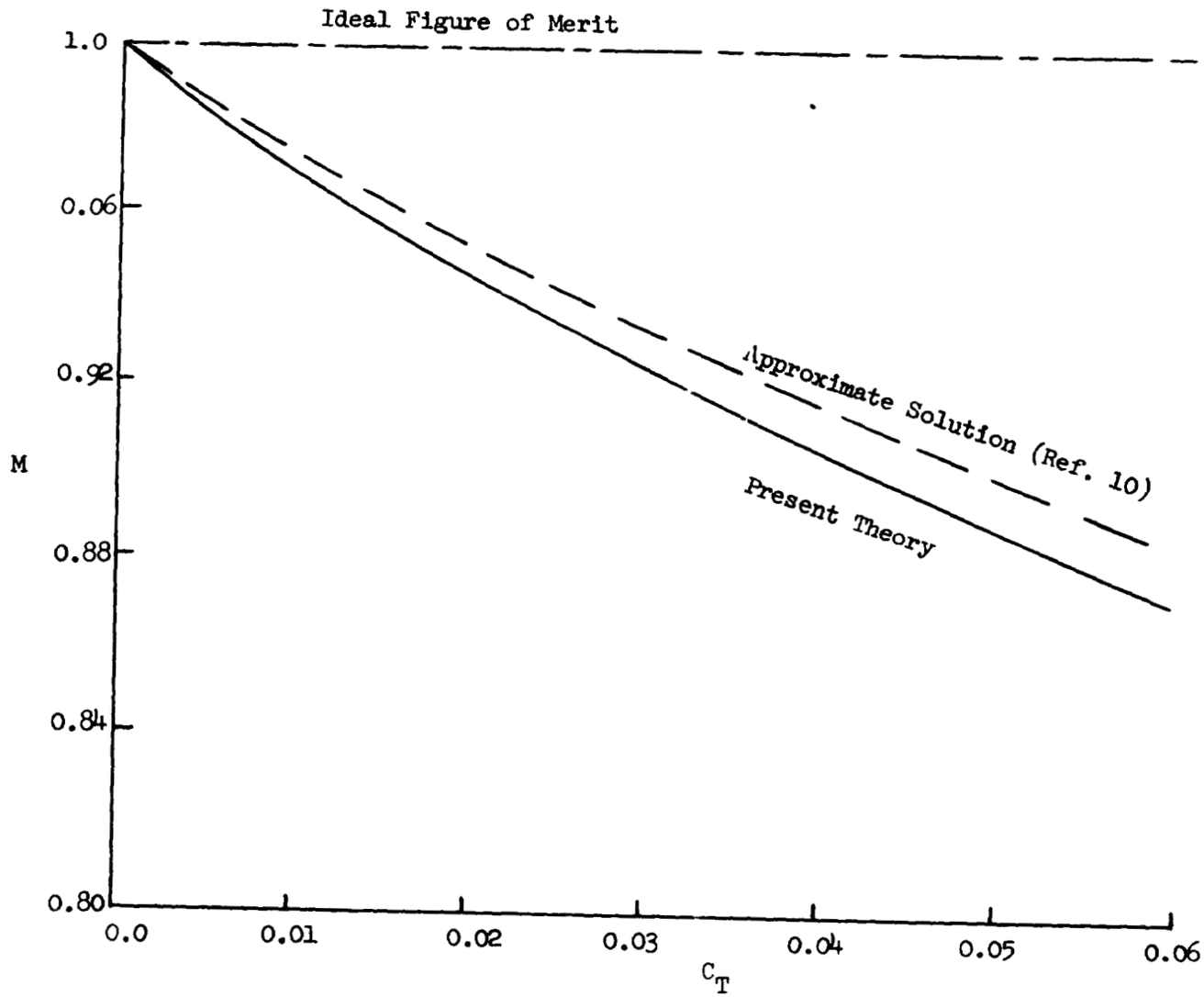

Figure 5. Optimum Figure of Merit

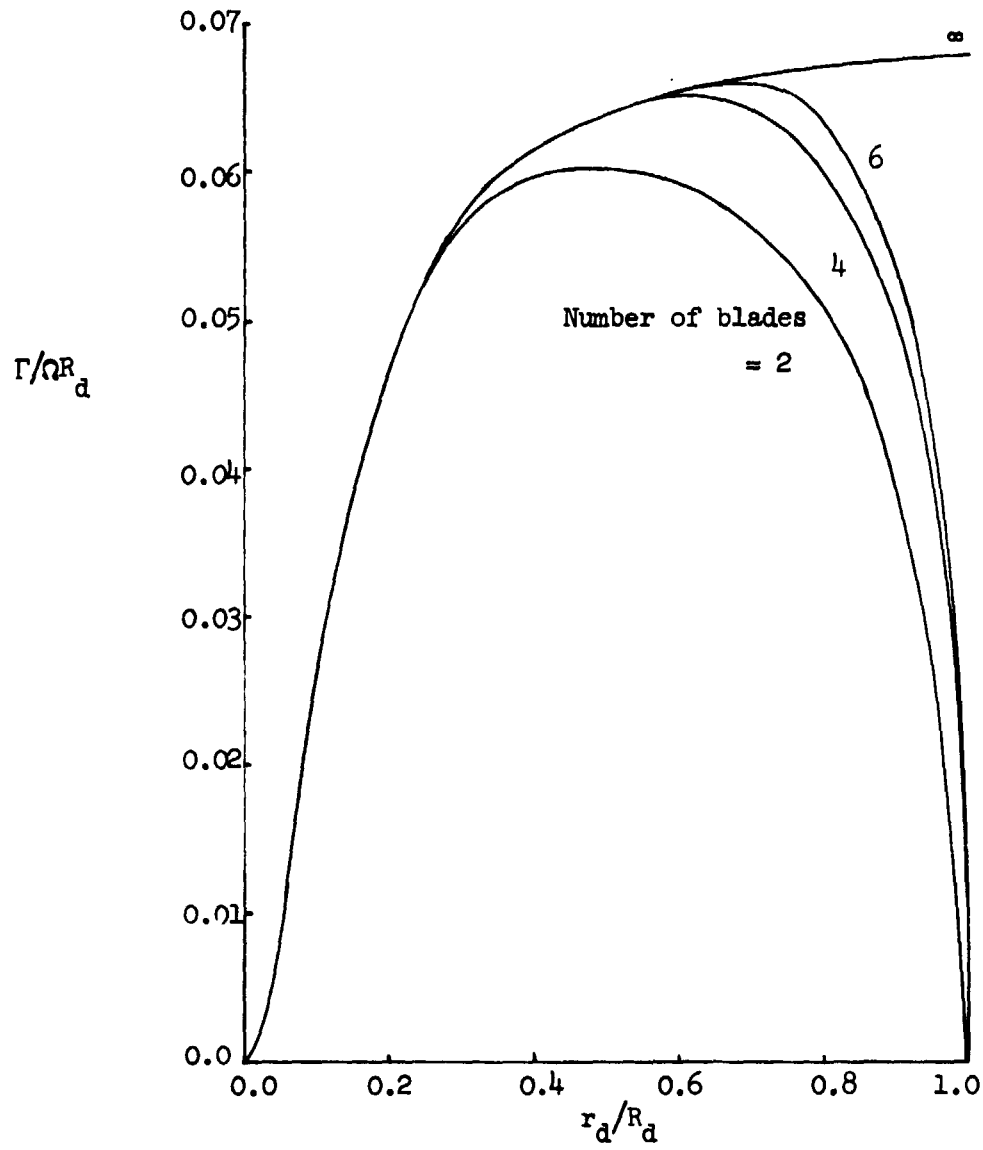

Figure 6. Effect of Number of Blades on the Distribution of Circulation - $C_T = 0.01$

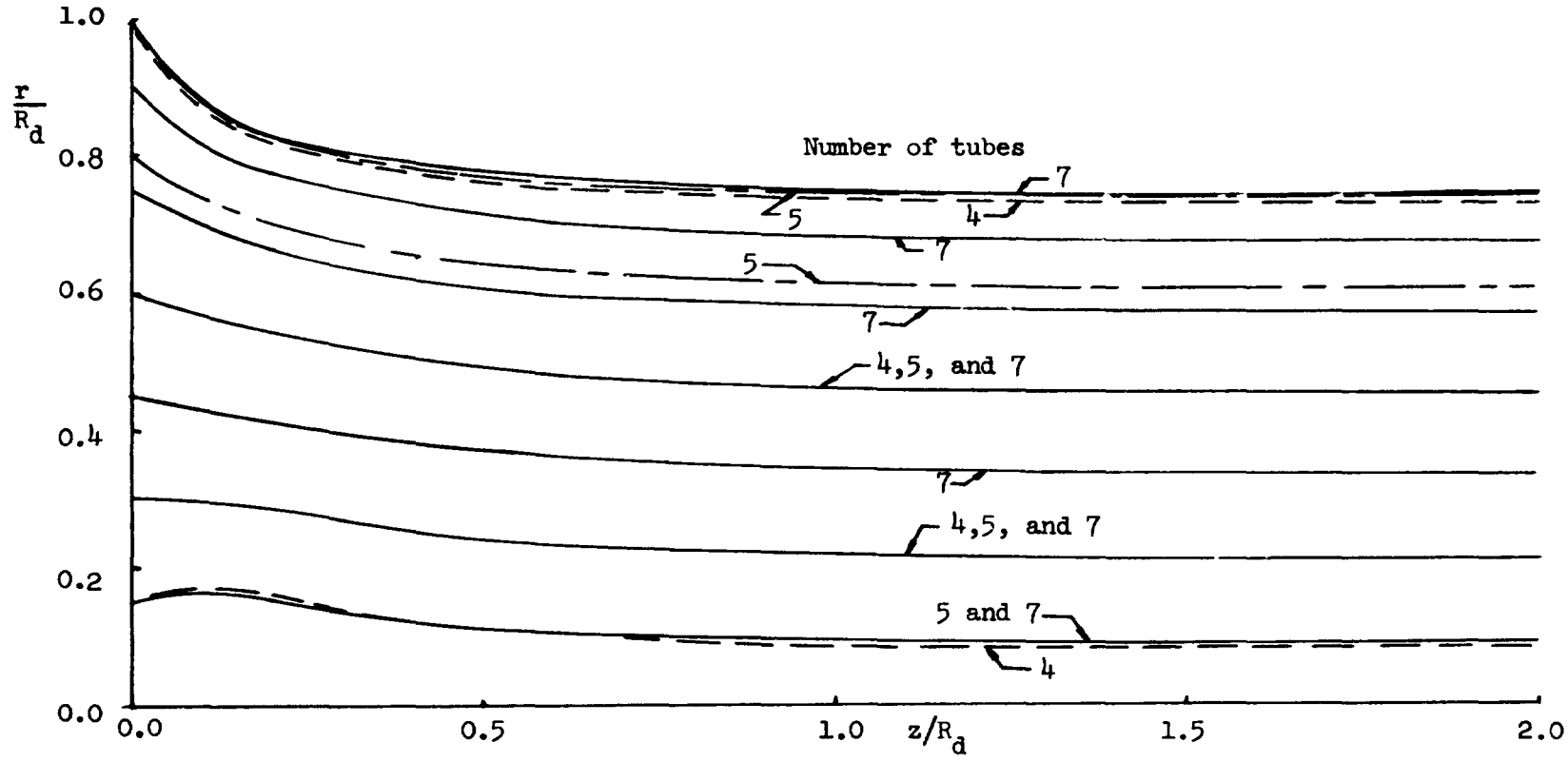

Figure 7. Comparison of Streamtube Shapes using 4, 5 and 7 Piecewise Constant Segments of Circulation

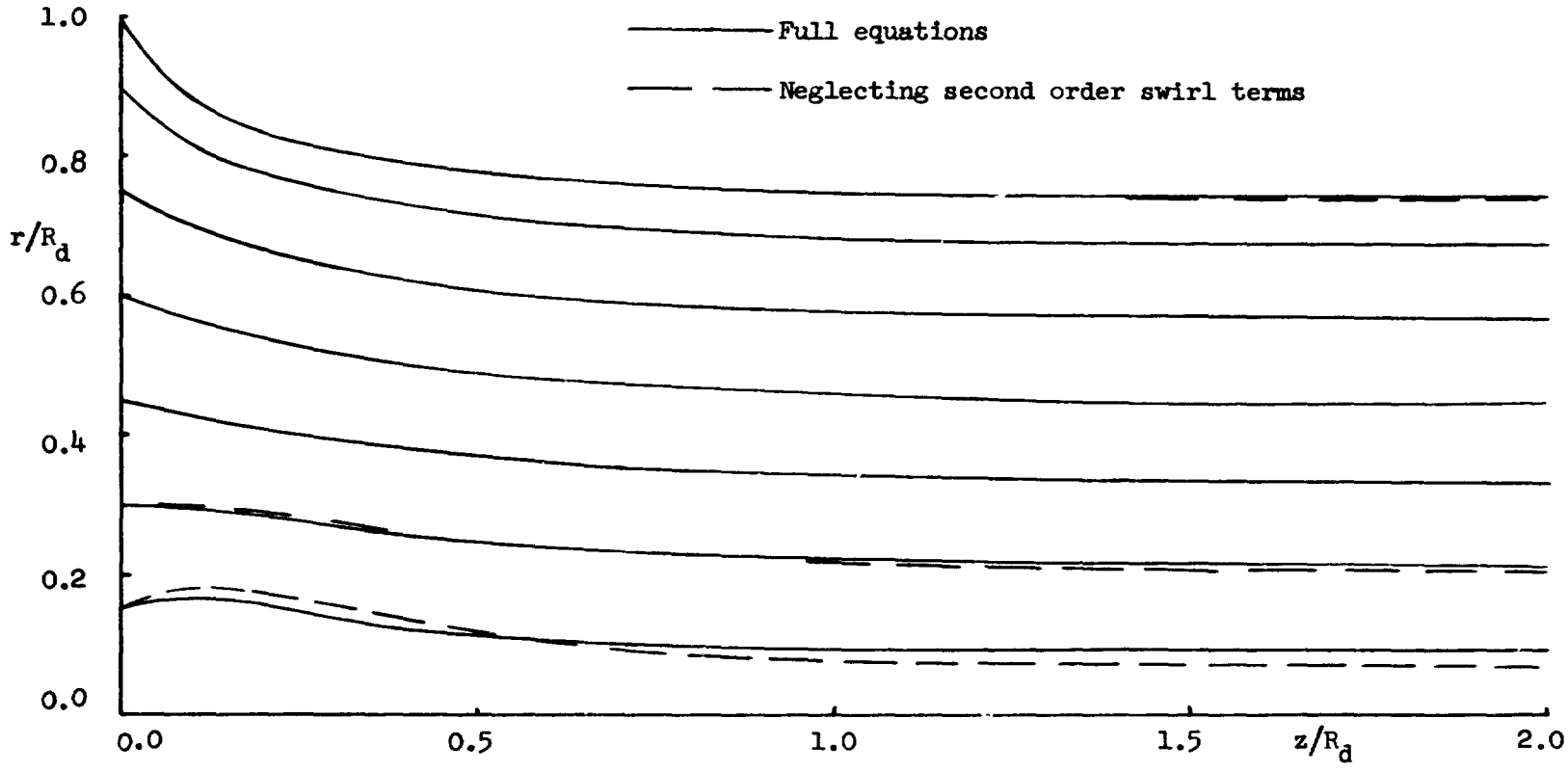

Figure 8. Effect of Second Order "Swirl" Terms on the Streamtube Shape for $C_T = 0.01$

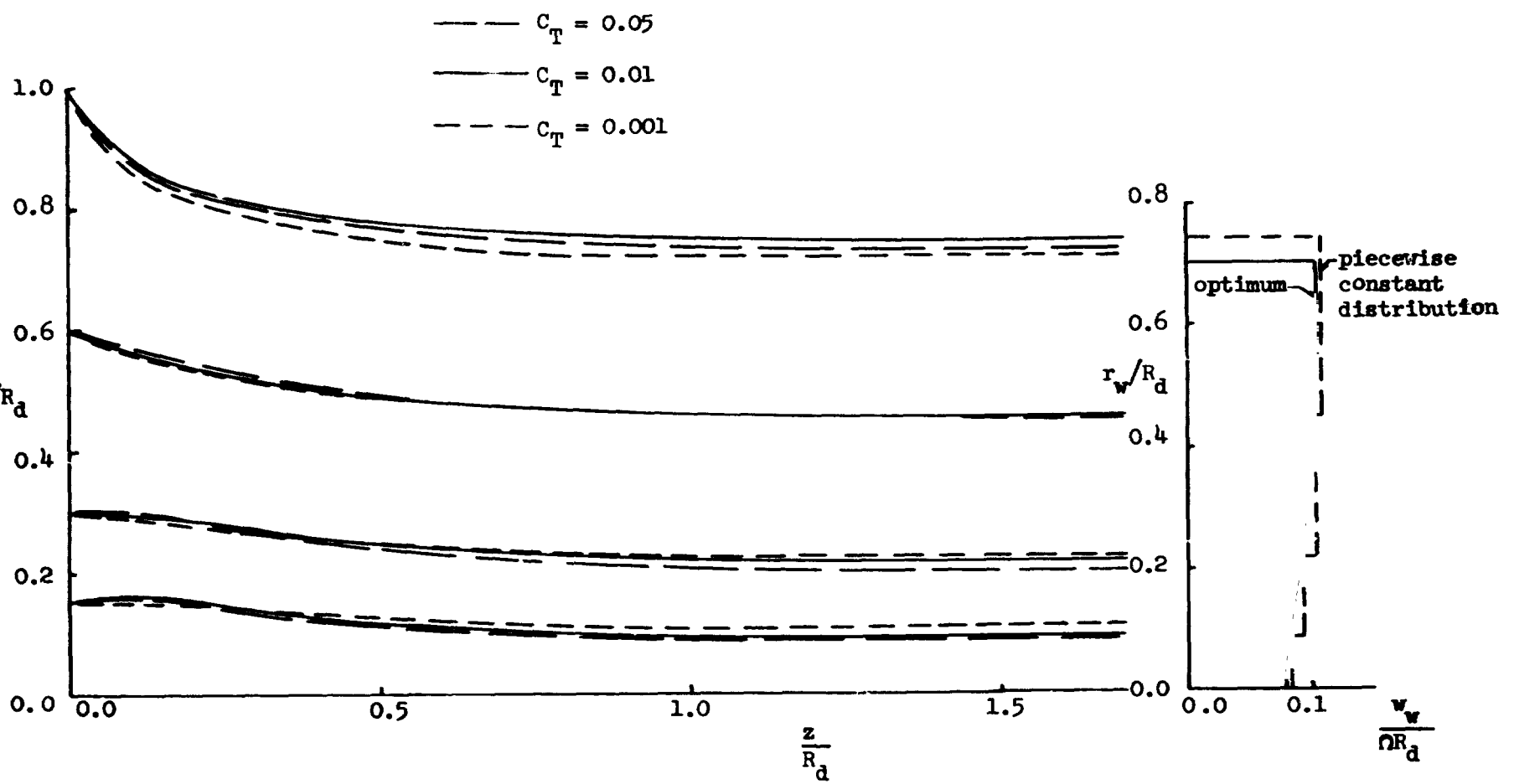

Figure 9. Streamtube Shapes for Various Values of the Thrust Coefficient and a Comparison of the Optimum and Piecewise Constant Axial Velocities in the Ultimate Wake for C_T = 0.01

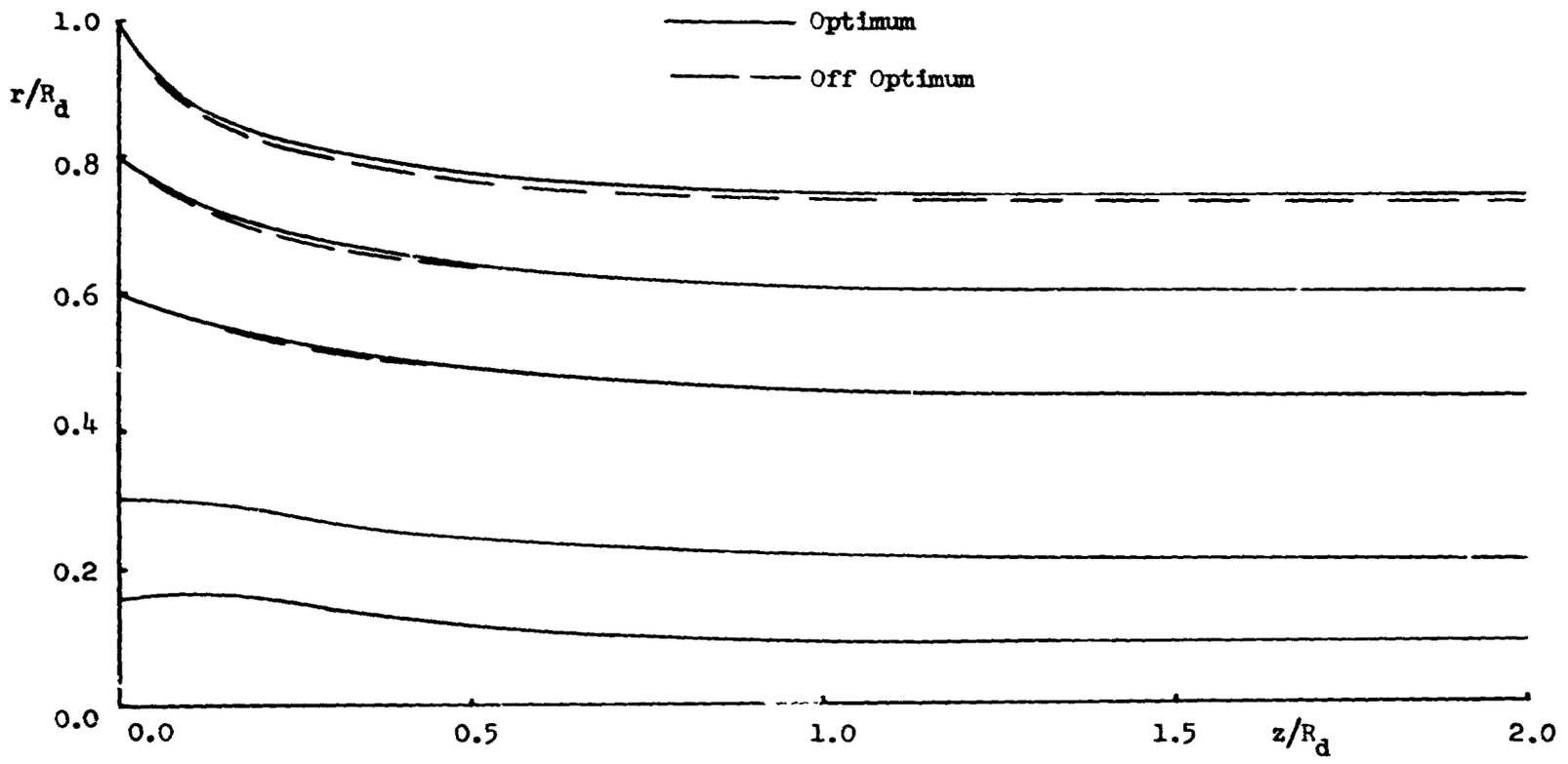

Figure 10. Streamtube Shapes for Optimum and Off-Optimum Circulation Distributions
$C_T = 0.01$

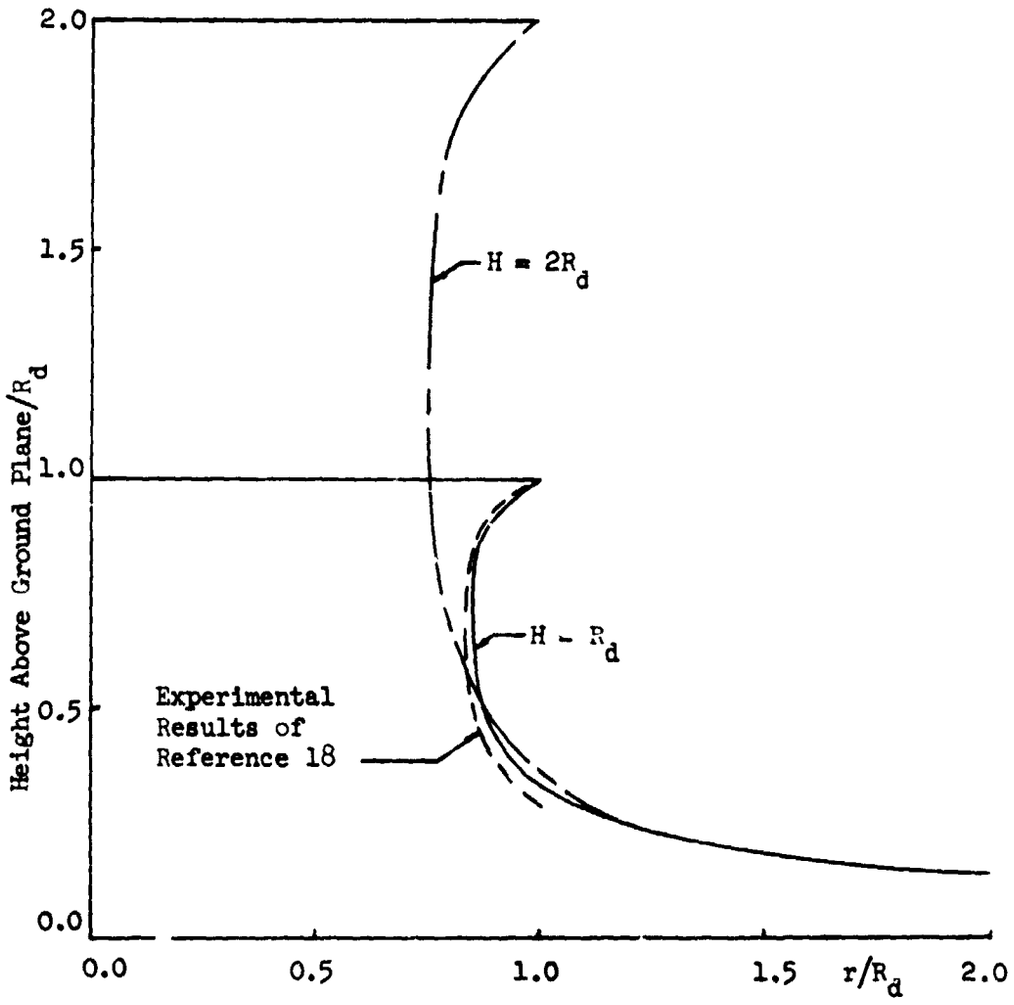

Figure 11. Slipstream Boundary Shapes for Rotors Hovering in Ground Effect at Heights of R_d and $2R_d$

APPENDIX A

EXPLICIT FORMULAE FOR AXI-SYMMETRIC VORTICES

In studies of flow fields induced by rotors and propellers, information about velocity components and stream functions associated with various axi-symmetric distributions of vortices is frequently required. In the course of the present study, explicit formulae for the velocity components and stream functions have been developed for several important distributions of axi-symmetric vortices. The availability of these explicit formulae facilitates the computation of the flow field associated with rotors and propellers. Selected formulae considered to be of general interest are presented in this Appendix. Of equal, perhaps even greater, utility is the approach developed for the derivation of these explicit formulae. This approach can be easily used to obtain explicit formulae for many additional distributions of axi-symmetric vortices. The approach is described in this Appendix. It is worth noting that analogous problems involving axi-symmetric distributions of singularities exist in many other fields of study such as electrostatics, magnetostatics, and potential flows about axi-symmetric bodies. The approach described here is easily adapted to these analogous problems. For example, as an offspring of the present study, explicit formulae for the velocity components due to sources of uniform strength distributed over a circular cylindrical segment were obtained (Ref. 32) and utilized in conjunction with the A. M. O.

Smith method (Ref. 33) for computing potential flows associated with lift-fan inflow.

It is well known that formulae for axi-symmetric flows frequently involve complete elliptic integrals. Complete elliptic integrals of the first, the second, and the third kinds are respectively defined as

$$K(k) = \int_0^{\frac{\pi}{2}} \frac{d\alpha}{(1 - k^2 \sin^2 \alpha)^{\frac{1}{2}}} \tag{A-1}$$

$$E(k) = \int_0^{\frac{\pi}{2}} (1 - k^2 \sin^2 \alpha)^{\frac{1}{2}} \, d\alpha \tag{A-2}$$

and

$$\Pi (n\backslash k) = \int_0^{\frac{\pi}{2}} \frac{d\alpha}{(1 - n \sin^2 \alpha)(1 - k^2 \sin^2 \alpha)^{\frac{1}{2}}} \tag{A-3}$$

The behavior of the complete elliptic integrals are well understood. Tabulated values as well as computational formulae for these integrals are available in standard handbooks of mathematical functions. Explicit formulae in terms of the complete elliptic integrals are therefore convenient formulae to employ in numerical procedures. Many definite integrals involving sines and/or cosines of the variable of integration are expressible in terms of the complete elliptic integrals. For example, the integral

$$I_1(k) = \int_0^{\frac{\pi}{2}} \frac{\sin^2 \alpha \cos^2 d\alpha}{(1 - k^2 \sin^2 \alpha)^{3/2}} = \int_0^{\frac{\pi}{2}} \frac{(\sin^2 \alpha - \sin^4 \alpha) \, d\alpha}{(1 - k^2 \sin^2 \alpha)^{3/2}}$$

may be reexpressed, upon integrating by parts, as

$$I_1(k) = \frac{1}{k^2} \int_0^{\frac{\pi}{2}} \frac{(2 \sin^2 \alpha - 1)\, d\alpha}{(1 - k^2 \sin^2 \alpha)^{\frac{1}{2}}}$$

$$= \frac{1}{k^2} \left[\frac{(2 - k^2)}{k^2} \int_0^{\frac{\pi}{2}} \frac{d\alpha}{(1 - k^2 \sin \alpha)^{\frac{1}{2}}} - \frac{2}{k^2} \int_0^{\frac{\pi}{2}} (1 - k^2 \sin^2 \alpha)^{\frac{1}{2}}\, d\alpha \right]$$

Thus one has

$$\int_0^{\frac{\pi}{2}} \frac{(\sin^2 \alpha - \sin^4 \alpha)\, d\alpha}{(1 - k^2 \sin^2 \alpha)^{3/2}} = \frac{1}{k^4} \left[(2 - k^2)\, K(k) - 2E(k) \right] \qquad \text{(A-4)}$$

As another example, consider the integral

$$I_2 = \int_0^{2\pi} \frac{\cos \beta\, d\beta}{(\tilde{a} - \tilde{b} \cos \beta)^{3/2}}$$

By letting $\beta = 2(\alpha + \pi/2)$ and recognizing that the resulting integrand is symmetric about $\alpha = 0$, one obtains

$$I_2 = \frac{4}{(\tilde{a} + \tilde{b})^{3/2}} \int_0^{\frac{\pi}{2}} \frac{(2 \sin^2 \alpha - 1)\, d\alpha}{(1 - k^2 \sin^2 \alpha)^{3/2}} \qquad \text{(A-5)}$$

where

$$k = \left(\frac{2\tilde{b}}{\tilde{a} + \tilde{b}} \right)^{\frac{1}{2}} \qquad \text{(A-6)}$$

Rearranging the integrand of Eq. (A-5) gives

$$I_2 = \frac{4}{(\tilde{a} + \tilde{b})^{3/2} k^2 (1 - k^2)} \left[(2 - 2k^2 + k^4) \int_0^{\frac{\pi}{2}} \frac{d\alpha}{(1 - k^2 \sin^2 \alpha)^{1/2}} \right.$$

$$\left. - (2 - k^2) \int_0^{\frac{\pi}{2}} (1 - k^2 \sin^2 \alpha)^{\frac{1}{2}}\, d\alpha \right.$$

$$- k^4 (2 - k^2) \int_0^{\frac{\pi}{2}} \frac{(\sin^2 \alpha - \sin^4 \alpha)\, d\alpha}{(1 - k^2 \sin^2 \alpha)^{3/2}} \Bigg]$$

Using Eqs. (A-1), (A-2), and (A-4), one then obtains

$$\int_0^{2\pi} \frac{\cos \beta \, d\beta}{(\tilde{a} - \tilde{b} \cos \beta)^{3/2}}$$

$$= \frac{4}{(\tilde{a} + \tilde{b})^{3/2} k^2} \left[- 2K(k) + \left(\frac{2 - k^2}{1 - k^2} \right) E(k) \right] \qquad \text{(A-7)}$$

Circular Vortex Filament

The velocity $d\vec{q}$ due to an element of vortex filament $d\vec{s}$ is given by the Biot-Savart Law:

$$d\vec{q} = \frac{\varkappa}{4\pi} \frac{(\vec{r}' - \vec{r}) \times d\vec{s}}{|\vec{r}' - \vec{r}|^3} \tag{A-8}$$

where $\varkappa$ is the strength of the vortex filament, $\vec{r}'$ is the position vector of the vortex filament, and $\vec{r}$ is the position vector of the observation point where $d\vec{q}$ is evaluated.

In a cylindrical coordinate system (r, θ, z), with a symmetric distribution of vorticity about the z-axis, it is easy to show that the r and z velocity components, u and w, are dependent only on the θ-component of vorticity, η. Thus the basic building block for the computation of u and w are the velocities and the stream functions associated with circular vortex filaments. These quantities associated with a circular vortex filaments shall be designated by the subscript "f".

Consider a circular vortex filament of strength $\varkappa$ and radius R centered about the z-axis in the z = Z plane. Since u_f and v_f are independent of θ, one obtains from Eq. (A-8)

$$u_f(r, z; R, Z) = \frac{\varkappa R(z - Z)}{4\pi} \int_0^{2\pi} \frac{\cos \theta' \, d\theta'}{[r^2 + R^2 - 2rR \cos \theta' + (z - Z)^2]^{3/2}} \tag{A-9}$$

and

$$w_f(r, z; R, Z) = \frac{\varkappa R}{4\pi} \int_0^{2\pi} \frac{(R - r \cos \theta') \, d\theta'}{[r^2 + R^2 - 2rR \cos \theta' + (z - Z)^2]^{3/2}} \tag{A-10}$$

Equation (A-9) yields, with the use of Eq. (A-7),

$$u_f(r, z; R, Z) = \frac{\kappa(z - Z)}{2\pi r \delta}\left[\frac{2 - k^2}{2(1 - k^2)} E(k) - K(k)\right] \qquad (A\text{-}11)$$

where

$$\delta = [(r + R)^2 + (z - Z)^2]^{\frac{1}{2}} \qquad (A\text{-}12)$$

and

$$k = \frac{2(rR)^{\frac{1}{2}}}{\delta} \qquad (A\text{-}13)$$

By writing the integral in Eq. (A-10) in terms of the integrals in Eqs. (A-1), (A-2), and (A-4), one similarly obtains from Eq. (A-10)

$$w_f(r, z; R, Z) = \frac{\kappa}{2\pi\delta}\left[\frac{2r - (r + R)k^2}{2r(1 - k^2)} E(k) + K(k)\right] \qquad (A\text{-}14)$$

The stream function Ψ_f due to the circular vortex filament is given by

$$\Psi_f(r, z; R, Z) = \int_o^r r' w_f(r', z; R, z)\, dr' \qquad (A\text{-}15)$$

where we have set $\Psi_f(o, z; R, Z)$ to be zero.

Instead of placing Eq. (A-14) into Eq. (A-15) and performing the integration with respect to r', it is simpler to use Eq. (A-10) and integrate first respect to r'. Thus, one writes

$$\Psi_f(r, z; R, Z) = \frac{\kappa R}{4\pi}\int_o^{2\pi}\int_o^r \frac{(Rr' - r'^2 \cos\theta')\, d\theta' dr'}{[r'^2 + R^2 - 2r'R\cos\theta' + (z - Z)^2]^{3/2}}$$

$$= - \frac{\varkappa R}{4\pi} \int_0^{2\pi} d\theta' \int_0^r \frac{\cos\theta'\, dr'}{[r'^2 + R^2 - 2r'R\cos\theta' + (z - Z)^2]^{\frac{1}{2}}}$$

$$- \frac{\varkappa R}{4\pi} \int_0^{2\pi} d\theta' \int_0^r \frac{\cos\theta' [2Rr'\cos\theta' - R^2 - (z - Z)^2] - Rr'}{[r'^2 + R^2 - 2r'R\cos\theta' + (z - Z)^2]^{3/2}} dr' \quad \text{(A-16)}$$

Integrating the first double integral by parts with respect to θ' gives

$$- \frac{\varkappa R}{4\pi} \int_0^{2\pi} d\theta' \int_0^r \frac{Rr'\sin^2\theta'\, dr'}{[r'^2 + R^2 - 2r'R\cos\theta' + (z - Z)^2]^{3/2}}$$

One then obtains

$$\Psi_f(r, z; R, Z) = - \frac{\varkappa R}{4\pi} \int_0^{2\pi} d\theta' \int_0^r \frac{\cos\theta'[Rr'\cos\theta' - R^2 - (z - Z)^2]dr'}{[r'^2 + R^2 - 2r'R\cos\theta' + (z - Z)^2]^{3/2}}$$

$$= \frac{\varkappa rR}{4\pi} \int_0^{2\pi} \frac{\cos\theta'\, d\theta'}{[r^2 + R^2 - 2rR\cos\theta' + (z - Z)^2]^{\frac{1}{2}}} \quad \text{(A-17)}$$

Letting $\theta' = 2(\alpha + \pi/2)$, one has

$$\int_0^{2\pi} \frac{\cos\theta'\, d\theta'}{[r^2 + R^2 - 2rR\cos\theta' + (z - Z)^2]^{\frac{1}{2}}} = \frac{4}{\delta} \int_0^{\frac{\pi}{2}} \frac{(2\sin^2\alpha - 1)\, d\alpha}{(1 - k^2\sin^2\alpha)^{\frac{1}{2}}}$$

$$= \frac{2k}{(rR)^{\frac{1}{2}}} \left[\left(\frac{2}{k^2} - 1 \right) K(k) - \frac{2}{k^2} E(k) \right] \quad \text{(A-18)}$$

Therefore

$$\Psi_f(r, z; R, Z) = \frac{\kappa\delta}{4\pi} \{(2 - k^2) K(k) - 2 E(k) \} \qquad (A\text{-}19)$$

The velocity components u and w associated with various axi-symmetrically distributed vortices are expressible as integrals involving u_f and w_f. Consider, as an example, a distribution of circular vortices of constant strength λ over the surface of a circular cylinder of radius R centered about the z-axis and extending between the planes $z = z_1$ and $z = z_2$. The vortices are in the θ-direction and the velocity components u and w due to this distribution of vortices are expressible as:

$$u(r, z) = \lambda \int_{z_1}^{z_2} u_f(r, z; R, Z)\, dZ \qquad (A\text{-}20)$$

and

$$w(r, z) = \lambda \int_{z_1}^{z_2} w_f(r, z; R, Z)\, dZ \qquad (A\text{-}21)$$

Attempts have been made in the past to place Eqs. (A-11) and (A-14) into integrals similar to those appearing in Eqs. (A-20) and (A-21) and to obtain explicit formulae for u and w for various axi-symmetrically distributed vortices. Such attempts, however, have met only with limited success. In particular, very few formulae are available in the literature for the velocity components and stream functions for general field points. In the present work, an alternative approach was utilized and many new explicit formula were derived.

Cylindrical Vortices

Consider the uniform distribution of vortices over a finite circular cylindrical surface described earlier. The velocity components due to this distribution of vortices are, according to Eqs. (A-9), (A-10), (A-20), and (A-21):

$$u(r, z) = \frac{\lambda R}{4\pi} \int_{z_1}^{z_2} (z - Z)\, dZ \int_0^{2\pi} \frac{\cos \theta'\, d\theta'}{[r^2 + R^2 - 2rR \cos \theta' + (z - Z)^2]^{3/2}} \quad \text{(A-22)}$$

$$w(r, z) = \frac{\lambda R}{4\pi} \int_{z_1}^{z_2} dZ \int_0^{2\pi} \frac{(R - r \cos \theta')\, d\theta'}{[r^2 + R^2 - 2rR \cos \theta' + (z - Z)^2]^{3/2}} \quad \text{(A-23)}$$

Instead of using Eq. (A-11) to express the right side of Eq. (A-22) in terms of an integral involving complete elliptic integrals, the integration for (A-22) is performed first with respect to Z, yielding,

$$u(r, z) = \frac{\lambda R}{4\pi} \left[\int_0^{2\pi} \frac{\cos \theta'\, d\theta'}{[r^2 + R^2 - 2rR \cos \theta' + (z - z_2)^2]^{\frac{1}{2}}} \right.$$

$$\left. - \int_0^{2\pi} \frac{\cos \theta'\, d\theta'}{[r^2 + R^2 - 2rR \cos \theta' + (z - z_1)^2]^{\frac{1}{2}}} \right] \quad \text{(A-24)}$$

One therefore has, using Eq. (A-18),

$$u(r, z) = \frac{\lambda}{\pi} \left(\frac{R}{r} \right)^{\frac{1}{2}} \left[\left(\frac{1}{k_2} - \frac{k_2}{2} \right) K(k_2) - \frac{1}{k_2} E(k_2) \right.$$

$$- \left(\frac{1}{k_1} - \frac{k_1}{2} \right) K(k_1) + \frac{1}{k_1} E(k_1) \Big] \qquad \text{(A-25)}$$

where

$$k_1 = \left[\frac{4rR}{(r + R)^2 + (z - z_1)^2} \right]^{\frac{1}{2}} \qquad \text{(A-26)}$$

$$k_2 = \left[\frac{4rR}{(r + R)^2 + (z - z_2)^2} \right]^{\frac{1}{2}} \qquad \text{(A-27)}$$

Similarly, integrating with respect to Z, one obtains from Eq. (A-23)

$$w(r, z) = - \frac{\lambda R}{4\pi} \left\{ \int_o^{2\pi} \frac{(R - r \cos \theta')\,(z - z_2)\, d\theta'}{(r^2+R^2-2rR \cos \theta')[r^2+R^2-2rR \cos \theta' + (z - z_2)^2]^{\frac{1}{2}}} \right.$$

$$\left. - \int_o^{2\pi} \frac{(R - r \cos \theta')\,(z - z_1)\, d\,\theta'}{(r^2 + R^2 - 2rR \cos \theta')[r^2 + R^2 - 2rR \cos \theta' + (z - z_1)^2]^{\frac{1}{2}}} \right\} \qquad \text{(A-28)}$$

Noting that

$$\int_o^{2\pi} \frac{(R - r \cos \theta')\, d\, \theta'}{(r^2 + R^2 - 2r\, R \cos\theta')[r^2 + R^2 - 2rR \cos \theta' + (z - Z)^2]^{\frac{1}{2}}}$$

$$= \frac{4}{(r + R)^2\, \delta} \int_o^{\frac{\pi}{2}} \frac{(R + r - 2r \sin^2 \alpha)\, d\alpha}{(1 - n \sin^2 \alpha)(1 - k^2 \sin^2 \alpha)^{\frac{1}{2}}}$$

$$= \frac{k}{(r+R)^2(rR)^{\frac{1}{2}}} \left[\frac{(r+R)^2}{R} \int_0^{\frac{\pi}{2}} \frac{d\alpha}{(1 - k^2 \sin^2 \alpha)} \right.$$

$$\left. - \frac{(r^2 - R^2)}{R} \int_0^{\frac{\pi}{2}} \frac{d\alpha}{(1 - n \sin^2 \alpha)(1 - k^2 \sin^2 \alpha)^{\frac{1}{2}}} \right]$$

$$= \frac{k}{R(rR)^{\frac{1}{2}}} K(k) - \frac{(r - R)\, k}{R(r + R)(rR)^{\frac{1}{2}}} \Pi (n \backslash k) \qquad \text{(A-29)}$$

where

$$n = \frac{4rR}{(r + R)^2} \qquad \text{(A-30)}$$

one obtains

$$w(r, z) = \frac{\lambda}{4\pi(rR)^{\frac{1}{2}}} \left\{ (z - z_2)\, k_2 \left[\frac{r - R}{r + R} \Pi (n \backslash k_2) - K(k_2) \right] \right.$$

$$\left. - (z - z_1)\, k_1 \left[\frac{r - R}{r + R} \Pi (n \backslash k_1) - K(k_1) \right] \right\} \qquad \text{(A-31)}$$

Equations (A-21) and (A-27) are convenient explicit formulae to use in the computation of velocities induced by cylindrical vortex segments. In computing rotor induced flowfield, these formulae offer the possibility of representing the trailing vortex system in the slipstream by a set of vortex cylinder segments. The strength and radius of the vortex segments may be determined in such a way that the kinematic (Ψ = constant along each vortex tube) and the kinetic (force free) con-

ditions are satisfied.

The behavior of u and w as given by Eqs. (A-25) and (A-31) can be determined by examining the properties of the complete elliptic integrals. In particular, it can be shown that u is well behaved everywhere except at the ends of the cylinder, i.e. at r = R and z = z_1 or z_2, where it possesses a logarithmic singularity. w is well behaved except on the cylinder where it changes discontinuously by the amount λ across the cylinder.

Equations (A-25) and (A-31) yield directly a number of velocity formulae for specialized cases. Some of these specialized formulae have been studied by other investigators (Ref. 26, 31). These specialized formulae include that of the velocities on the cylinder of radius R itself, the velocities on and away from the cylinder due to a semi-infinite cylinder ($z_1 = 0$, $z_2 = \infty$), and that due to an infinite cylinder. The formulae presented here, i.e., Eqs. (A-25) and (A-31), can further be utilized to derive an explicit formula for the stream function. This formula for the stream function is also useful in axi-symmetric flowfield computations.

Consider, for the moment, a semi-infinite vortex cylinder of strength λ and radius R, centered about the z-axis and extending from $z = z_1$ to infinity. The velocity components induced by this semi-infinite vortex cylinder shall be designated u_1 and w_1. Equation (A-25) gives, with $z_2 = \infty$, $k_2 = 0$. Equation (A-25) therefore reduces to

$$u_1(r, z) = \frac{\lambda}{\pi}\left(\frac{R}{r}\right)^{\frac{1}{2}}\left[-\left(\frac{1}{k_1} - \frac{k_1}{2}\right)K(k_1) + \frac{1}{k_1}E(k_1)\right] \qquad \text{(A-32)}$$

Equation (A-3) gives

$$\Pi(n\backslash o) = \int_0^{\frac{\pi}{2}} \frac{d\alpha}{1 - n\sin^2\alpha} = \frac{\pi}{2}\left|\frac{R + r}{R - r}\right| \qquad \text{(A-33)}$$

Therefore, for $r < R$, Eq. (A-31) gives

$$w_1(r, z) = \frac{\lambda}{2} - \frac{\lambda(z - z_1)k_1}{4\pi(rR)^{\frac{1}{2}}}\left[\frac{r - R}{r + R}\Pi(n\backslash k_1) - K(k_1)\right]$$

and, for $z = z_1$ and $r < R$, one has

$$w_1(r, z_1) = \frac{\lambda}{2} \qquad \text{(A-34)}$$

The stream function Ψ_1 for this semi-infinite vortex cylinder can now be evaluated by using the relation

$$\Psi_1(r, z) = \int_0^r r'w(r', z_1)\,dr' - r\int_{z_1}^z u(r, z')\,dz' \qquad \text{(A-35)}$$

where the value of Ψ_1 is taken to be zero along the z-axis.

Placing Eqs. (A-32) and (A-34) into Eq. (A-35) and evaluating the first integral gives,

$$\Psi_1(r,z) = \frac{\lambda r^2}{4} + \frac{\lambda(rR)^{\frac{1}{2}}}{\pi}\int_{z_1}^z \left[\left(\frac{1}{k_1'} - \frac{k_1'}{2}\right)K(k_1') - \frac{1}{k_1'}E(k_1')\right]dz' \qquad \text{(A-36)}$$

where

$$k_1' = \left[\frac{4rR}{(r + R)^2 + (z' - z_1)^2} \right]^{\frac{1}{2}} \tag{A-37}$$

Equation (A-37) gives

$$dz' = - \frac{4rR\, dk_1'}{k_1'^2 [4rR - (r + R)^2 k_1'^2]^{\frac{1}{2}}} \tag{A-38}$$

Using Eqs. (A-1), (A-2), and (A-38), Eq. (A-36) is reexpressed as

$$\Psi_1(r, z) = \frac{\lambda r^2}{4} + \frac{\lambda (rR)^{3/2}}{\pi (r+R)} \int_n^{k_1^2} \frac{dx}{x(n - x)^{\frac{1}{2}}} \int_0^{\frac{\pi}{2}} \frac{(1 - 2 \sin^2\alpha) d\alpha}{(1 - x \sin^2 \alpha)^{\frac{1}{2}}} \tag{A-39}$$

Integrating by parts with respect to α gives

$$\Psi_1(r, z) = \frac{\lambda r^2}{4} - \frac{\lambda (rR)^{3/2}}{\pi (r + R)} \int_n^{k_1^2} \frac{dx}{(n - x)^{\frac{1}{2}}} \int_0^{\frac{\pi}{2}} \frac{\sin^2 \alpha \cos^2 \alpha\, d\alpha}{(1 - x \sin^2 \alpha)^{3/2}}$$

Integrating with respect to x then yields

$$\Psi_1(r, z) = \frac{\lambda r^2}{4} + \frac{\lambda (rR)^{\frac{1}{2}} n k_1 |z - z_1|}{2\pi} \int_0^{\frac{\pi}{2}} \frac{[\sin^2\alpha - \sin^4\alpha]\, d\alpha}{(1 - n \sin^2\alpha)(1 - k_1^2 \sin^2\alpha)^{\frac{1}{2}}}$$

The integral in the above equation can be expressed in terms of the complete elliptic integrals. One obtains, after some algebraic manipulations,

$$\Psi_1(r, z) = \frac{\lambda r^2}{4} + \frac{\lambda (rR)^{\frac{1}{2}} k_1 |z - z_1|}{2\pi} \left[\left(\frac{1}{k_1^2} + \frac{1 - n}{n} \right) \Pi(k_1) \right.$$

$$- \frac{1}{k_1^2} E(k_1) + \frac{n-1}{n} \Pi (n \backslash k_1) \Big] \qquad \text{(A-40)}$$

The stream function $\Psi_2(r, z)$ due to a semi-infinite vortex cylinder of strength λ and radius R extending from $z = z_2$ to infinity and centered about the z-axis is, from Eq. (A-40), obviously

$$\Psi_2(r, z) = \frac{\lambda r^2}{4} + \frac{\lambda (rR)^{\frac{1}{2}} k_2 |z - z_2|}{2\pi} \Big[\left(\frac{1}{k_2^2} + \frac{1-n}{n} \right) K(k_2)$$

$$- \frac{1}{k_2} E(k_2) + \frac{n-1}{n} \Pi (n \backslash k_2) \Big] \qquad \text{(A-41)}$$

By the use of the principle of superposition, one then obtains the following formula for the stream function $\Psi(r, z)$ due to a finite vortex cylinder of strength λ and radius R centered about the z-axis and extending between the planes z_1 and z_2:

$$\Psi(r, z) = \Psi_1(r, z) - \Psi_2(r, z)$$

or

$$\Psi(r, z) = \frac{\lambda (rR)^{\frac{1}{2}}}{2\pi} \Big\{ k_1 |z - z_1| \Big[\left(\frac{1}{k_1^2} + \frac{1-n}{n} \right) K(k_1)$$

$$- \frac{1}{k_1^2} E(k_1) + \frac{n-1}{n} \Pi (n \backslash k_1) \Big]$$

$$- k_2 |z - z_2| \Big[\left(\frac{1}{k_2^2} + \frac{1-n}{n} \right) K(k_2) - \frac{1}{k_2^2} E(k_2) + \frac{n-1}{n} \Pi (n \backslash k_2) \Big] \Big\} \qquad \text{(A-42)}$$

For cylindrical vortices with a non-uniform distribution of strength, explicit formulae for the velocity components and for the stream function can be obtained by utilizing the approach and the results presented above. For example, with a linear distribution of vorticity strength, λ, i.e.,

$$\lambda = \lambda_1 + \lambda_2 z \tag{A-43}$$

where λ_1 and λ_2 are constants, the velocity components and the stream function are each expressible as a sum of two parts, one part due to λ_1 and the other part due to $\lambda_2 z$. The part due to λ_1 has already been expressed in terms of the complete elliptic integrals [Eqs. (A-25), (A-31), and (A-42)]. To demonstrate the procedure for establishing expressions for the part due to $\lambda_2 z$, consider the radial velocity u_ℓ.

$$u_\ell(r, z) = \frac{\lambda_2 R}{4\pi} \int_{z_1}^{z_2} Z(z - Z)\, dZ \int_0^{2\pi} \frac{\cos\theta'\, d\theta'}{[r^2 + R^2 - 2rR\cos\theta' + (z - Z)^2]^{3/2}} \tag{A-44}$$

Equation (A-44) may be rewritten as

$$u_\ell(r,z) = \frac{\lambda_2 R}{4\pi} \int_{z_1}^{z_2} dZ \int_0^{2\pi} \frac{(r^2 + R^2 - 2r\,R\cos\theta')\cos\theta'\, d\theta'}{[r^2 + R^2 - 2r\,R\cos\theta' + (z - Z)^2]^{3/2}}$$

$$+ \frac{\lambda_2 Rz}{4\pi} \int_{z_1}^{z_2} (z - Z)\, dZ \int_0^{2\pi} \frac{\cos\theta'\, d\theta'}{[r^2 + R^2 - 2rR\cos\theta' + (z - Z)^2]^{3/2}}$$

$$- \frac{\lambda_2 R}{4\pi} \int_{z_1}^{z_2} dZ \int_0^{2\pi} \frac{\cos\theta'\, d\theta'}{[r^2 + R^2 - 2rR\cos\theta' + (z - Z)^2]^{\frac{1}{2}}} \tag{A-45}$$

The double integrals in Eq. (A-45) can be readily expressed in terms of the complete elliptic integrals using the approach presented earlier. In particular, the first double integral is easily expressed in terms of the complete elliptic integrals by first performing the integration with respect to Z. The second double integral is identical to that appearing in Eq. (A-22), which has been expressed in terms of the complete elliptic integrals [Eq. (A-25)]. The third double integral is easily shown to be equivalent to the second integral appearing in Eq. (A-35), which again has been expressed in terms of the complete elliptic integrals.

Annular Vortices

Consider a distribution of circular vortices of strength λ_3/R, where λ_3 is a constant, over an annular surface in the $z = Z$ plane. The surface extends from $r = r_1$ to $r = r_2$.

The velocity components due to this annular vortex surface are, according to Eqs. (A-9) and (A-10), given by

$$u(r, z) = \frac{\lambda_3(z - Z)}{4\pi} \int_{r_1}^{r_2} dR \int_o^{2\pi} \frac{\cos\theta' \, d\theta'}{[r^2 + R^2 - 2rR\cos\theta' + (z - Z)^2]^{3/2}} \quad \text{(A-46)}$$

$$w(r, z) = \frac{\lambda_3}{4\pi} \int_{r_1}^{r_2} dR \int_o^{2\pi} \frac{(R - r\cos\theta') \, d\theta'}{[r^2 + R^2 - 2rR\cos\theta' + (z - Z)^2]^{3/2}} \quad \text{(A-47)}$$

Integrating with respect to R gives

$$u(r,z) = \frac{\lambda_3(z-Z)}{4\pi} \left[\int_o^{2\pi} \frac{\cos\theta' \, (r_2 - r\cos\theta') \, d\theta'}{[r^2+(z-Z)^2 - r^2\cos^2\theta'] \, [r^2 + r_2^2 - 2rr_2\cos\theta' + (z-Z)^2]^{\frac{1}{2}}} \right.$$

$$\left. - \int_o^{2\pi} \frac{\cos\theta'(r_1 - r\cos\theta') \, d\theta'}{[r^2 + (z-Z)^2 - r^2\cos^2\theta'] \, [r^2 + r_1^2 - 2\,rr_1\cos\theta' + (z - Z)^2]^{\frac{1}{2}}} \right] \quad \text{(A-48)}$$

$$w(r, z) = -\frac{\lambda_3}{4\pi} \int_o^{2\pi} \frac{d\theta'}{[r^2 + R^2 - 2\,r\,R\cos\theta' + (z - Z)^2]^{\frac{1}{2}}} \quad \text{(A-49)}$$

It is easy to show, by letting $\theta' = 2(\alpha + \pi/2)$ and using partial fractions, that

$$\int_0^{2\pi} \frac{\cos\theta'\,(R - r\cos\theta')\,d\theta'}{[r^2 + (z - Z)^2 - r^2\cos^2\theta'][r^2 + R^2 - 2rR\cos\theta' + (z - Z)^2]^{\frac{1}{2}}}$$

$$= \frac{4}{(z-Z)^2[(r + R)^2 + (z-Z)^2]^{\frac{1}{2}}} \int_0^{\frac{\pi}{2}} \frac{(2\sin^2\alpha - 1)(R + r - 2r\sin^2\alpha)d\alpha}{(1-m_1\sin^2\alpha)(1 + m_2\sin^2\alpha)(1-k^2\sin^2\alpha)^{\frac{1}{2}}}$$

$$= \frac{4}{(z - Z)^2[(r + R)^2 + (z - Z)^2]^{\frac{1}{2}}} \left\{ \frac{(z - Z)^2}{r} \int_0^{\frac{\pi}{2}} \frac{d\alpha}{(1 - k^2\sin^2\alpha)^{\frac{1}{2}}} \right.$$

$$- \left[\frac{(z - Z)^2}{2r} - \frac{R + r}{m_2} \right] \int_0^{\frac{\pi}{2}} \frac{d\alpha}{(1 - m_1\sin^2\alpha)(1 - k^2\sin^2\alpha)^{\frac{1}{2}}}$$

$$\left. - \left[\frac{(z - Z)^2}{2r} + \frac{R + r}{m_1} \right] \int_0^{\frac{\pi}{2}} \frac{d\alpha}{(1 + m_2\sin^2\alpha)(1 - k^2\sin^2\alpha)^{\frac{1}{2}}} \right\} \quad \text{(A-50)}$$

where

$$m_1 = \frac{2r}{[r^2 + (z - Z)^2]^{\frac{1}{2}} + r} \quad \text{(A-51)}$$

and

$$m_2 = \frac{2r}{[r^2 + (z - Z)^2]^{\frac{1}{2}} - r} \quad \text{(A-52)}$$

Using Eqs. (A-1), (A-3), (A-44) and (A-48), one then obtains

$$u(r, z) = \frac{\lambda_3 (z - Z)}{8\pi r^{3/2}} \left\{ \frac{k_{r_2}}{r_2^{\frac{1}{2}}} \left[4K(k_{r_2}) - \left(2 - \frac{r_2 + r}{r} m_1 \right) \Pi(m_1 \backslash k_{r_2}) \right. \right.$$

$$\left. - \left(2 - \frac{r_2 + r}{r} m_2 \right) \Pi (- m_2 \backslash k_{r_2}) \right]$$

$$- \frac{k_{r_1}}{r_1^{\frac{1}{2}}} \left[4K(k_{r_1}) - \left(2 - \frac{r_1 + r}{r} m_1 \right) \Pi (m_1 \backslash k_{r_1}) \right.$$

$$\left. \left. - \left(2 + \frac{r_1 + r}{r} m_2 \right) \Pi (- m_2 \backslash k_{r_1}) \right] \right\} \qquad \text{(A-53)}$$

where

$$k_{r_1} = \left[\frac{4rr_1}{(r + r_1)^2 + (z - Z)^2} \right]^{\frac{1}{2}} \qquad \text{(A-54)}$$

and

$$k_{r_2} = \left[\frac{4rr_2}{(r + r_2)^2 + (z - Z)^2} \right]^{\frac{1}{2}} \qquad \text{(A-55)}$$

It is easy to show that Eq. (A-45) gives

$$w(r, z) = - \frac{\lambda_3}{2\pi r^{\frac{1}{2}}} \left[\frac{k_{r_2}}{r_2^{\frac{1}{2}}} K(k_{r_2}) - \frac{k_{r_1}}{r_1^{\frac{1}{2}}} K(k_{r_1}) \right] \qquad \text{(A-56)}$$

According to Eq. (A-17), the stream function due to the annular vortex surface is given by

$$\psi(r, z) = \frac{\lambda_3 r}{4\pi} \int_{r_1}^{r_2} dR \int_c^{2\pi} \frac{\cos\theta' \, d\theta'}{[r^2 + R^2 - 2rR\cos\theta' + (z - Z)^2]^{\frac{1}{2}}} \quad \text{(A-57)}$$

Integrating by parts with respect to θ' yields

$$\psi(r, z) = \frac{\lambda_3 r^2}{4\pi} \int_{r_1}^{r_2} dR \int_o^{2\pi} \frac{R \sin^{-2}\theta' \, d\theta'}{[r^2 + R^2 - 2rR\cos\theta' + (z - Z)^2]^{3/2}}$$

$$= \frac{\lambda_3 r^2}{4\pi} \int_o^{2\pi} \frac{[\cos\theta' \, rR - r^2 - (z-Z)^2] \sin^2\theta' \, d\theta'}{[r^2 + (z-Z)^2 - r^2\cos^2\theta'][r^2 + R^2 - 2rR\cos\theta' + (z-Z)^2]^{\frac{1}{2}}} \Bigg|_{R = r_1}^{r_2} \quad \text{(A-58)}$$

The last integral in Eq. (A-58) can be re-expressed as

$$\frac{16}{\delta(z - Z)^2} \int_o^{\frac{\pi}{2}} \frac{[2rR\sin^2\alpha - rR - r^2 - (z - Z)^2](\sin^2\alpha - \sin^4\alpha) \, d\alpha}{(1 - k^2\sin^2\alpha)^{\frac{1}{2}} (1 - m_1\sin^2\alpha)(1 + m_2\sin^2\alpha)}$$

$$= \frac{2}{\delta r^2} \left\{ [R^2 - r^2 - (z - Z)^2] K(k) - [(R + r)^2 + (z - Z)^2] E(k) \right.$$

$$\left. + \frac{2r^2}{m_2} \left(\frac{2}{m_2} + 1 - \frac{R}{r} \right) \Pi(m_1 \backslash k) + \frac{2r^2}{m_1} \left(\frac{2}{m_1} - 1 + \frac{R}{r} \right) \Pi(-m_2 \backslash k) \right\}$$

Therefore, one obtains from Eq. (A-58)

$$\psi(r, z) = \frac{\lambda_3}{2\pi} \left(\frac{1}{[(r + r_2)^2 + (z - Z)^2]^{\frac{1}{2}}} \left\{ [r_2^2 - r^2 - (z - Z)^2] K(k_{r_2}) \right. \right.$$

$$\left. \left. - [(r_2 + r)^2 + (z - Z)^2] E(k_{r_2}) \right.\right.$$

$$+ \frac{2r^2}{m_2}\left(\frac{2}{m_2} + 1 - \frac{r_2}{r}\right)\Pi(m_1\backslash k_{r_2}) + \frac{2r^2}{m_1}\left(\frac{2}{m_1} - 1 + \frac{r_2}{r}\right)\Pi(-m_2\backslash k_{r_2})\Big\}$$

$$- \frac{1}{[(r + r_1)^2 + (z - Z)^2]^{\frac{1}{2}}}\Big\{[r_1^2 - r^2 - (z - Z)^2]\,K(k_{r_1})$$

$$- [(r_1 + r)^2 + (z - Z)^2]\,E(k_{r_1})$$

$$+ \frac{2r^2}{m_2}\left(\frac{2}{m_2} + 1 - \frac{r_1}{r}\right)\Pi\,(m_1\backslash k_{r_1})$$

$$+ \frac{2r^2}{m_1}\left(\frac{2}{m_1} - 1 + \frac{r_1}{r}\right)\Pi\,(-m_2\backslash k_{r_1})\Big\}\Big) \qquad \text{(A-59)}$$

It is clear that the approach described here permits explicit formulae for the velocity components and stream function to be obtained for other types of distribution of vortices in annular regions.

APPENDIX B

OPTIMUM PERFORMANCE OF ROTORS AND PROPELLERS IN AXIAL FLIGHT

Equations relating the thrust and the power of rotors or propellers in axial flight to the velocity components in the ultimate wake can be established rigorously by a simple extension of the analysis of Chapter IV. They are:

$$P = \rho\Omega \int_{S_1} v_w \, w_w \, r_w \, ds_w \tag{B-1}$$

and

$$T = \tfrac{1}{2}\rho \int_{S_1} [(w_w - w_\infty)^2 + (2\Omega r_w - v_w) \, v_w] \, ds_w \tag{B-2}$$

where w_∞ is the ascent speed of the rotor or the advance speed of the propeller.

The relation between the axial and tangential velocity components in the ultimate wake, which also can be established rigorously by an extension of the analysis of Chapter IV, is:

$$\frac{w_w^2}{2} = \Omega \, v_w \, r_w + \frac{w_\infty^2}{2} - \frac{v_w^2}{2} + \int_{r_w}^{R_w} \frac{v_w^2}{r} \, dr \tag{B-3}$$

Following the approach described in Chapter IV, a perturbation Δv_w in the tangential velocity is introduced at $r_w = a$ and the resulting

changes in the axial velocity distribution, the power, and the thrust, are sought. It is obvious from Eq. (B-3) that the relation between the tangential velocity perturbation and the change in the axial velocity distribution is not altered by the presence of a non-zero speed of advance. Consequently, since Eq. (B-1) also is independent of w_∞, the expression for the change in power previously developed for the hovering rotor is applicable to the present case of a non-zero speed of advance. One therefore has

$$\Delta P = 2\pi\rho\Omega\epsilon\,\Delta r_w\, a^3 \left\{ \frac{v_{wa}}{w_{wa}} (\Omega a - v_{wa}) + w_{wa} + \frac{2v_{wa}}{a^3} \int_0^a \frac{v_w r_w^2 dr_w}{w_w} \right\} \tag{B-4}$$

The change in thrust is dependent on w_∞ and is

$$\Delta T = 2\pi\rho\epsilon\,\Delta r_w\, a^2 \left\{ 2\Omega a - v_{wa} - \frac{w_\infty}{w_{wa}} (\Omega a - v_{wa}) - \frac{2v_{wa} w_\infty}{a^2} \int_0^a \frac{r dr}{w_w} \right\} \tag{B-5}$$

Equations (B-4) and (B-5) may be combined to express ΔP in the form

$$\Delta P = h(a)\ \Delta T \tag{B-6}$$

where $h(a)$ is a function only of a, the location where the tangential

velocity perturbation is introduced. Following the analysis of Chapter IV, the criterion for optimum performance is that h(a) is a constant, independent of a. In other words, the criterion for optimum performance is

$$\int_0^{r_w} \frac{(rv_w + Nw_\infty)\, rdr}{w_w} = \frac{r_w^2}{2v_w} \left[N(2\Omega r_w - v_w) - r_w w_w - \frac{r_w v_w + Nw_\infty}{w_w} (\Omega r_w - v_w)\right] \qquad \text{(B-7)}$$

where N is a constant.

It is easy to show that, upon setting $w_\infty = 0$, Eq. (B-7) reduces to the optimum performance criterion previously obtained for the hovering rotor.

A differential form of the optimum performance criterion is obtained by differentiating both sides of Eq. (B-7) with respect to r_w. The resulting equation relates the derivatives dv_w/dr_w and dw_w/dr_w. Differentiating Eq. (B-3) with respect to r_w yields a second equation relating dv_w/dr_w and dw_w/dr_w. After some algebraic manipulations, one then obtains the following two first order differential equations:

$$\frac{d\tilde{w}_w}{d\tilde{r}_w} = 2\tilde{w}_w \tilde{v}_w(\tilde{r}_w - \tilde{v}_w)[2\tilde{w}_w^2 \tilde{r}_w - \tilde{N}(4\tilde{r}_w - \tilde{v}_w)\tilde{w}_w + 2\Lambda\tilde{N}\tilde{r}_w + 2\tilde{v}_w\tilde{r}_w^2]/F \qquad \text{(B-8)}$$

$$\frac{d\tilde{v}_w}{d\tilde{r}_w} = \tilde{v}_w \{3\tilde{w}_w^4 \tilde{r}_w - 2\tilde{N}\tilde{w}_w^3(3\tilde{r}_w - \tilde{v}_w)$$

$$+ [3\Lambda\tilde{N}\tilde{r}_w + \tilde{v}_w\tilde{r}_w(5\tilde{r}_w - 2\tilde{v}_w)]\,\tilde{w}_w^2$$

$$- [\tilde{N}\Lambda + \tilde{v}_w\tilde{r}_w]\,\tilde{v}_w(\tilde{r}_w - \tilde{v}_w)^2\ \}/F \qquad \text{(B-9)}$$

where

$$F = \tilde{w}_w^4 r_w^2 - 2\tilde{N}\tilde{w}_w^3\tilde{r}_w^2 + [\Lambda\tilde{N}\tilde{r}_w^2 - \tilde{v}_w\tilde{r}_w(\tilde{r}_w - 2\tilde{v}_w)]\tilde{w}_w^2$$

$$+ (\Lambda\tilde{N} - \tilde{v}_w\tilde{r}_w)\,\tilde{v}_w\,(\tilde{r}_w - \tilde{v}_w)^2\,\tilde{r}_w \qquad \text{(B-10)}$$

$\Lambda = w_\infty/\Omega R_w$ is a non-dimensional advance speed, $\tilde{w}_w$ and $\tilde{v}_w$ are velocity components non-dimensionalized with reference to ΩR_w, $\tilde{r}_w$ and $\tilde{N}$ are non-dimensional r_w and N with reference to R_w.

At the rim of the ultimate wake, Eq. (B-3) gives

$$\frac{\tilde{w}_{w_o}^2}{2} = \frac{\Lambda^2}{2} + \tilde{v}_{w_o}(2 - \tilde{v}_{w_o}) \qquad \text{(B-11)}$$

Taking the upper limit of the integral in Eq. (B-7) to be R_w, one obtains

$$N = \frac{\Lambda^2 + \tilde{v}_{w_o}\left[3 - 2\tilde{v}_{w_o} + 2\tilde{w}_{w_o}\int_o^1 \frac{\tilde{r}_w^2\tilde{v}_w}{\tilde{w}_w}\,d\tilde{r}_w\right]}{\tilde{w}_{w_o}\left[2 - \tilde{v}_{w_o} - \Lambda(1 - \tilde{v}_{w_o})/\tilde{w}_{w_o} - 2\Lambda\,\tilde{v}_{w_o}\int_o^1 \frac{\tilde{r}_w\,d\tilde{r}_w}{\tilde{w}_w}\right]} \qquad \text{(B-12)}$$

Equations (B-8) through (B-12) permit the computation of optimum

distributions $\tilde{v}_w$ and $\tilde{w}_w$ for any given values of $\tilde{N}$ and Λ, or, alternatively $\tilde{v}_{w_o}$ and Λ. An iterative method for computing $\tilde{v}_w$ and $\tilde{w}_w$ is described in Ref. 27 for various values of $\tilde{v}_{w_o}$. Sample results are presented in Ref. 30.

REFERENCES

1. Jenny, David S.; Olson, John R.; and Landgrebe, Anton J.; A Reassessment of Rotor Hovering Performance Prediction Methods, J. Am. Helicopter Soc., Vol. 13, No. 2, April 1968, p. 1.

2. Lerbs, H. W.; An Approximate Theory of Heavily Loaded, Free-Running Propellers in the Optimum Condition, Trans. Soc. Naval Arch. & Marine Engr., Vol. 58, 1950, p. 138.

3. Wu, T. Yao-Tsu; Flow Through a Heavily Loaded Actuator Disk, Schiffstechnik, Vol. 9, No. 47, 1962, p. 134.

4. Greenberg, M. D. and Kaskel, A. L.; Inviscid Flow Field Induced by a Rotor in Ground Effect, NASA CR-1027, 1968.

5. Greenberg, M. D. and Powers, S. R.; Nonlinear Actuator Disk Theory and Flow Field Calculations, Including Nonuniform Loading, NASA CR-1672, September, 1970.

6. Erickson, J. C.; A Continuous Vortex Sheet Representation of Deformed Wakes of Hovering Propellers, Proc. CAL/USAAVLABS Symp. of Aero. Problems Associated with V/STOL Aircraft, Vol. 1, 1969.

7. Landgrebe, A. J.; An Analytical Method for Predicting Rotor Wake Geometry, AIAA/AHS VTOL Research Design and Operations Meeting, AIAA Paper No. 69-196, February 1969.

8. Rankine, W. J. M.; On the Mechanical Principles of the Action of Propellers, Trans. Inst. Nav. Arch., Vol. 6, 1865, p. 13.

9. Froude, R. E.; On the Part Played in Propulsion by Difference of Fluid Pressure, Trans. Inst. Nav. Arch., Vol. 30, 1889, p. 390.

10. Glauert, H.; Airplane Propellers as Part L, Vol. IV: Aerodynamic Theory, W. F. Durand, Editor-in-Chief, Dover, 1963.

11. Prandtl, L.; Appendix to Schraubenpropeller mit geringstem Energieverlust, by Betz, Gottinger Nachr., 1919, p. 213.

12. Goldstein, S.; On Vortex Theory of Screw Propellers, Proc. Royal Soc. of London, Series, A, Vol. 63, April 1929, p. 440.

13. Lock, C. N. H.; The Application of Goldstein's Theory to the Practical Design of Aircrews, British Aero. Res. Comm. R & M No. 1377, 1931.

14. Theodorsen, T.; Theory of Propellers, McGraw-Hill, 1948.

15. Theodorsen, T.; Theory of Static Propellers and Helicopter Rotors, AHS Forum 1969.

16. Theodorsen, T.; The Theory of Propellers III - The Slipstream Contraction with Numerical Values for Two-Blade and Four Blade Propellers, NACA Rept. 777, 1944.

17. Lerbs, H. W.; Moderately Loaded Propellers with a Finite Number of Blades and an Arbitrary Distribution of Circulation. Trans. Soc. Naval Arch. & Marine Engr., Vol. 60, 1952, p. 73.

18. Gray, R. B.; Experimental Smoke and Electromagnetic Analog Study of Induced Flow Field about a Model Rotor in Steady Flight within Ground Effect, NACA TN D-458, August 1960.

19. Rorke, J. B. and Wells, C. D.; The Prescribed Wake-Momentum Analysis. Proceedings of the Third CAL/AVLABS Symposium on Aerodynamics of Rotary Wing and VTOL Aircraft, Vol. 1, May 1969.

20. Clark, D. R. and Leiper, A. C.; The Free Wake Analysis. AHS 25th Annual Forum, Paper No. 321, May 1969.

21. Gray, R. B. and Brown, G. W.; A Vortex Wake Analayis of a Single-Bladed Hovering Rotor and a Comparison with Experimental Data. AGARD-CP-111, February 1973.

22. Wu, J. C. and Thompson, J. F.; Numerical Solutions of Time-Dependent Incompressible Navier-Stokes Equations Using an Integro-Differential Formulation, Computers and Fluids, Vol. 1, pp. 197-215.

23. Chaplin, H. R.; A Method for Numerical Calculation of Slipstream Contraction of a Shrouded Impulse Disc in the Static Case with Application to other Axisymmetric Potential Flow Problems, DTMB Aero Report 1077, June 1964.

24. Cox, B. W.; Vortex Ring Solutions of Axisymmetric Propeller Flow Problems, MIT Dept. of Naval Arch. and Marine Eng. Report No. 68-13, May 1968.

25. Lamb, H.; Hydrodynamics, Dover Publications, New York, 1932.

26. Kuchemann, D. and Weber, J; Aerodynamics of Propulsion, McGraw-Hill, New York, 1953.

27. Wu, J. C., Sigman, R. K., and Goorjian, P. M.; Optimum Performance of Hovering Rotors, NASA TM X-62, 138, March, 1972.

28. Wu, J. C., Sigman, R. K. and Goorjian, P. M.; Optimum Performance of Static Propellers and Rotors. Developments in Theoretical and Applied Mechanics, Vol. 6, 1972.

29. Goorjian, P. M.; An Invalid Equation in the General Momentum Theory of the Actuator Disk, AIAA J., Vol. 10, No. 4, p. 543.

30. Summers, M. H.; Optimum Performance of Rotors in Vertical Flight, Unpublished Special Problem, Georgia Institute of Technology, 1972.

31. Hough, G. R. and Ordway, D. E.; The Steady Velocity Field of a Propeller with Constant Circulation Distribution, AHS Journal, Vol. 10, No. 2, 1965.

32. Wu, J. C., Sigman, R., Hubbartt, J., and McMahon, H.; Potential Flow Studies of Lift-Fan Inflow Interference Phenomena, Air Force Systems Command Rept. ARL 73-0132, October, 1973.

33. Hess, J. and Smith, A. M. O.; Calculation of Potential Flows about Arbitrary Bodies; Progress in Aeronautical Sciences, Vol. 8, Pergamon Press, 1967.